

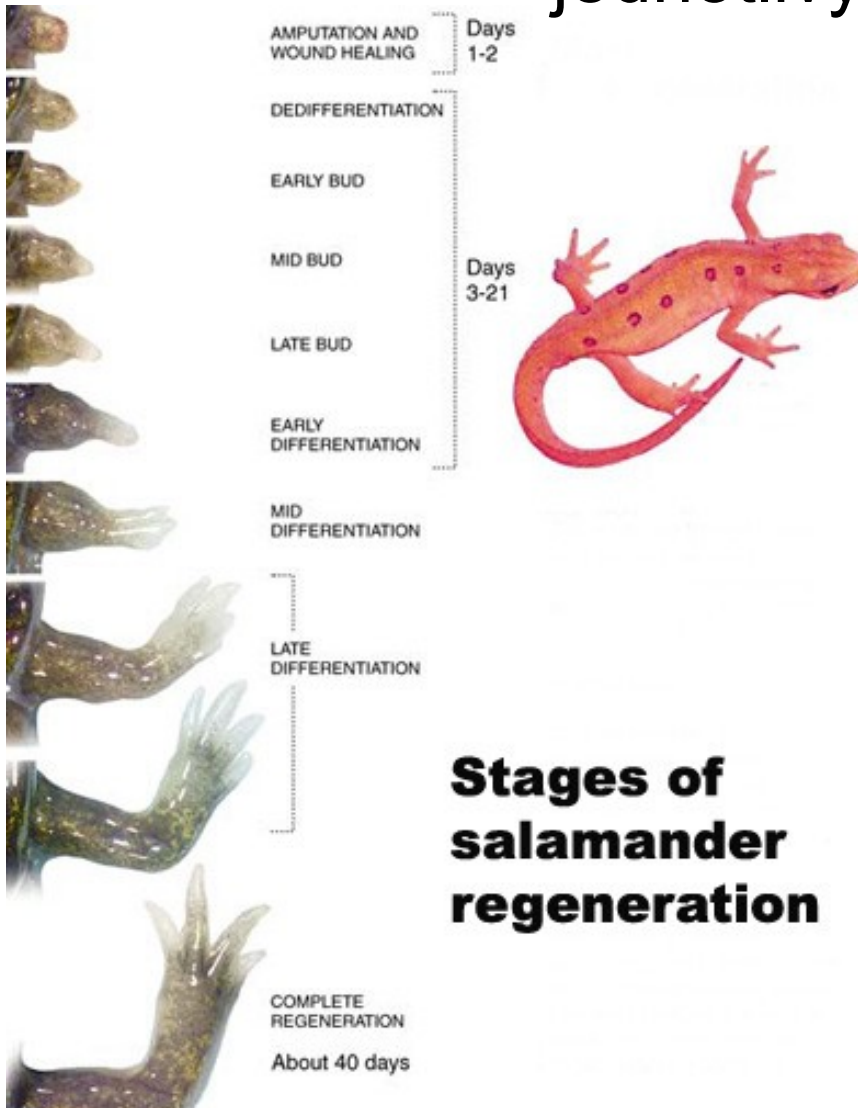
#6

Aktivace vývojových mechanismů
u dospělého organismu

Kdy a proč se reaktivují procesy spjaté s embryonálním vývojem?

- odpověď je logická: tehdy, když je potřeba znovu vytvářet struktury poškozené či zničené tj. když je potřeba regenerovat
- v lidském organismu běžně regenerují celé tkáně – např. vlasové kořínky (doba „života“ 3-4 roky), epitel střeva, epitel plic, krevní buňky nebo játra

přesto se Schopnosti regenerace se liší mezi jednotlivými organismy

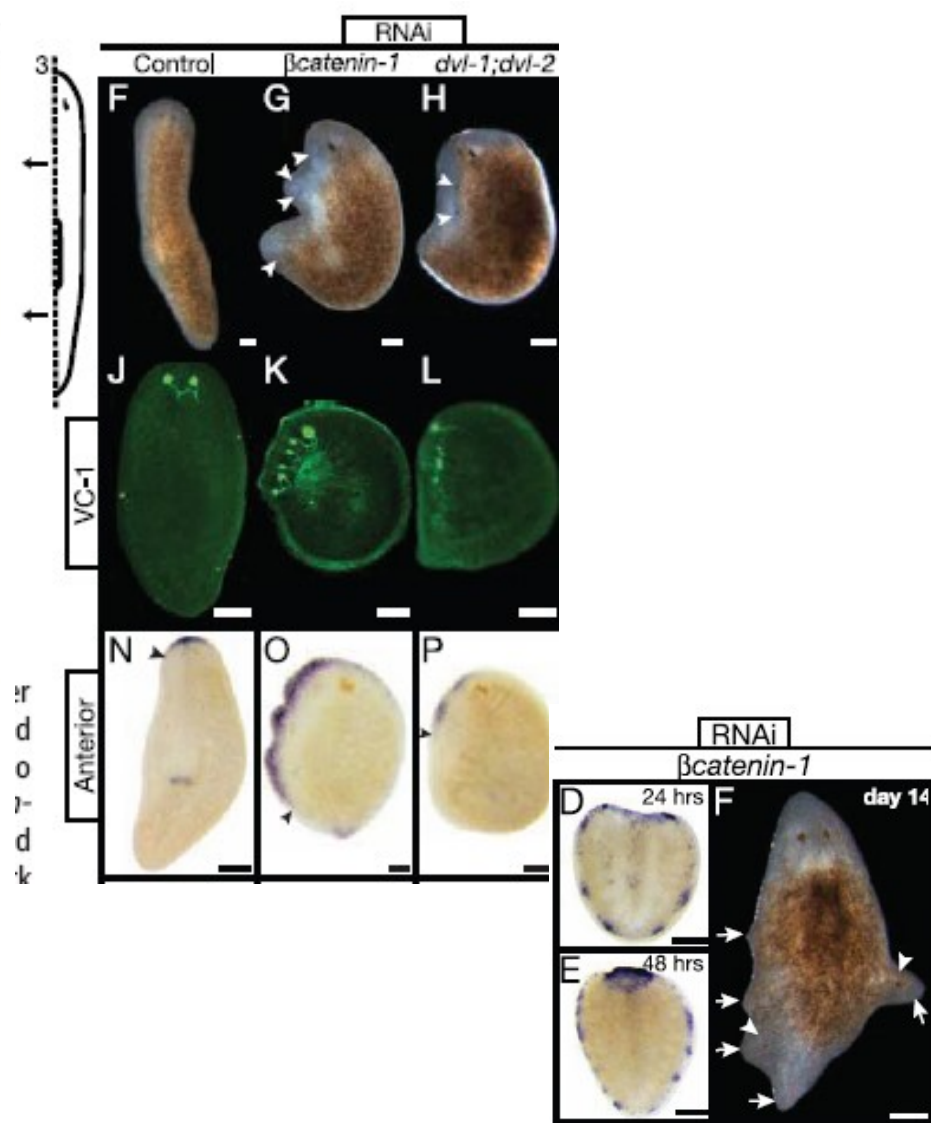
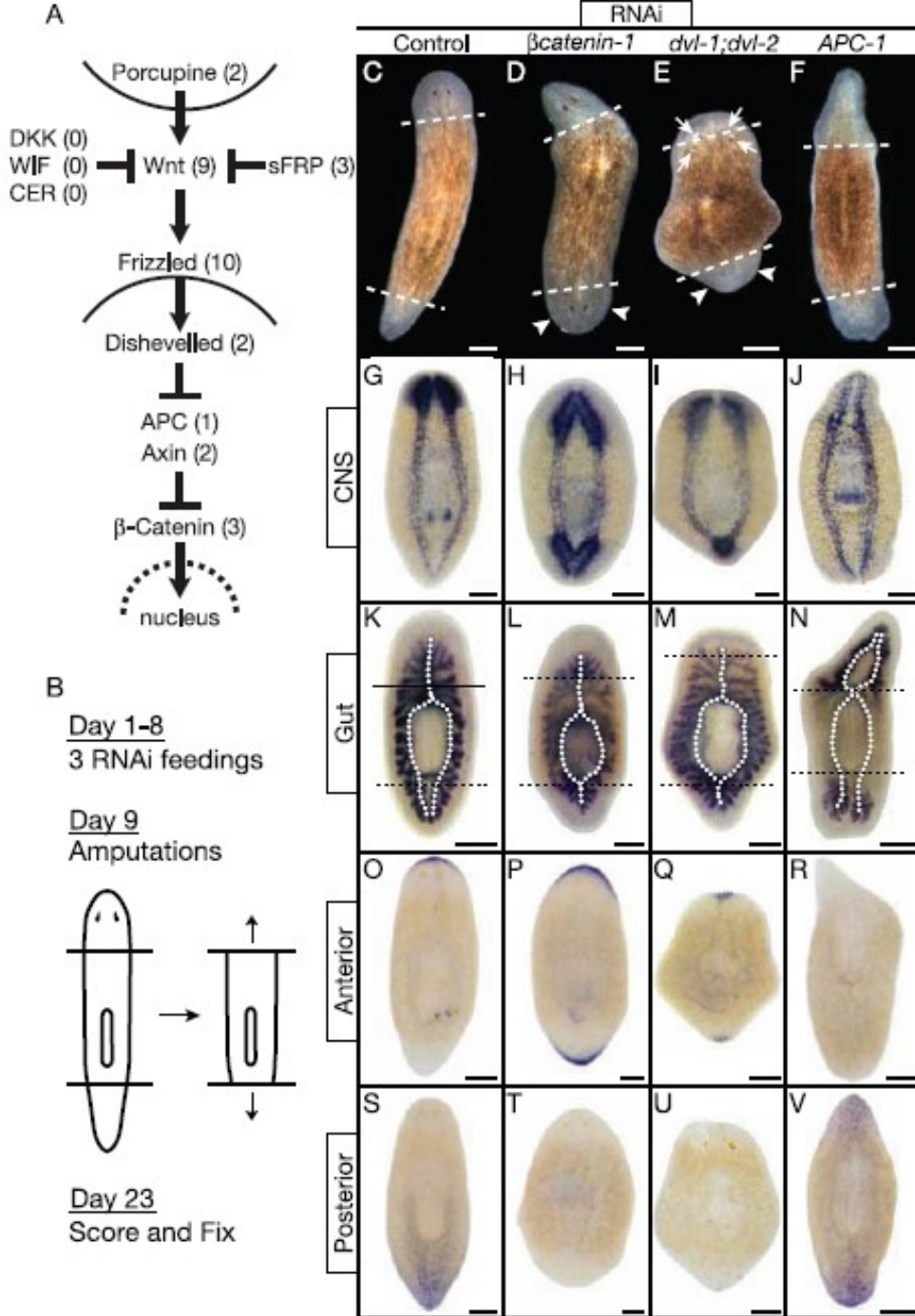


po amputaci



po 10 letech



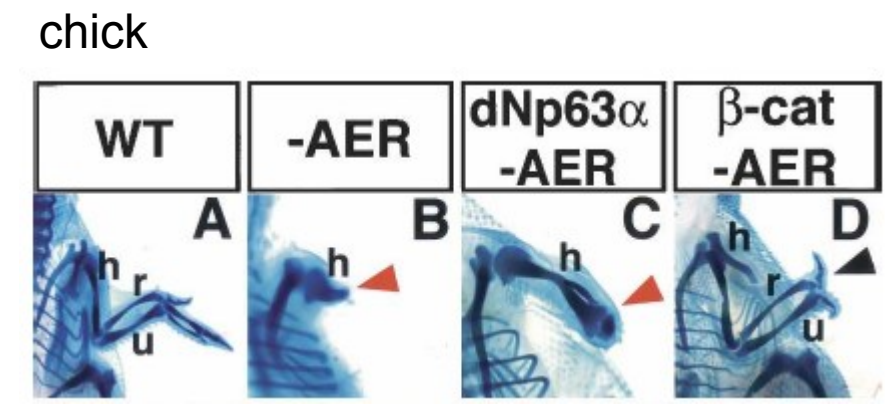
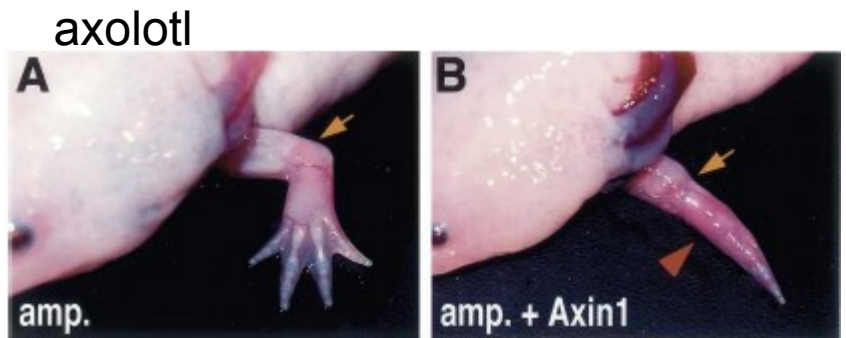


β-Catenin Defines Head Versus Tail Identity During Planarian Regeneration and Homeostasis

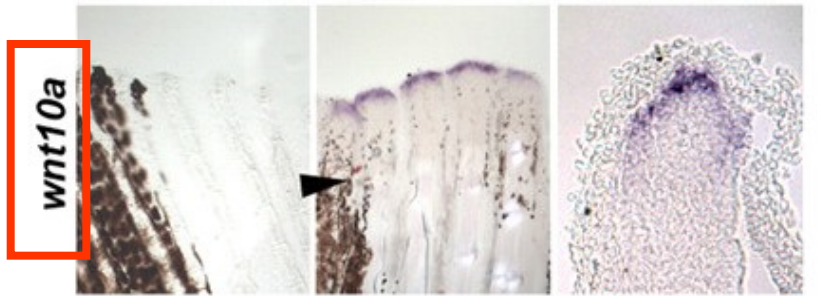
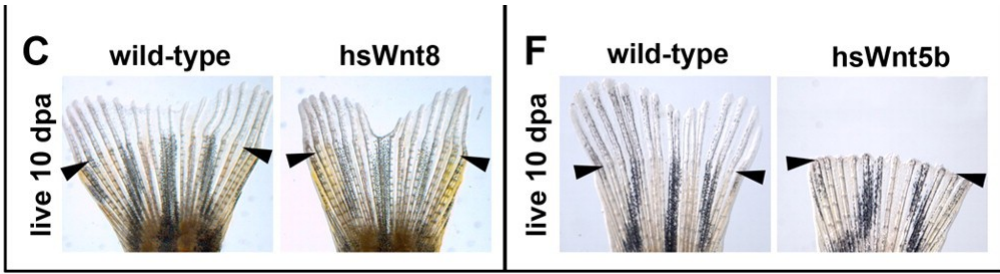
Kyle A. Gurley, Jochen C. Rink, Alejandro Sánchez Alvarado*

SCIENCE VOL 319 18 JANUARY 2008

Morphogenetic pathways (canonical Wnt signalling, Hedgehog, TGF, Notch) are required for regeneration in multiple organisms



zebrafish



Aktivace nádorových kmenových buněk jako důsledek chronického poškození a regenerace

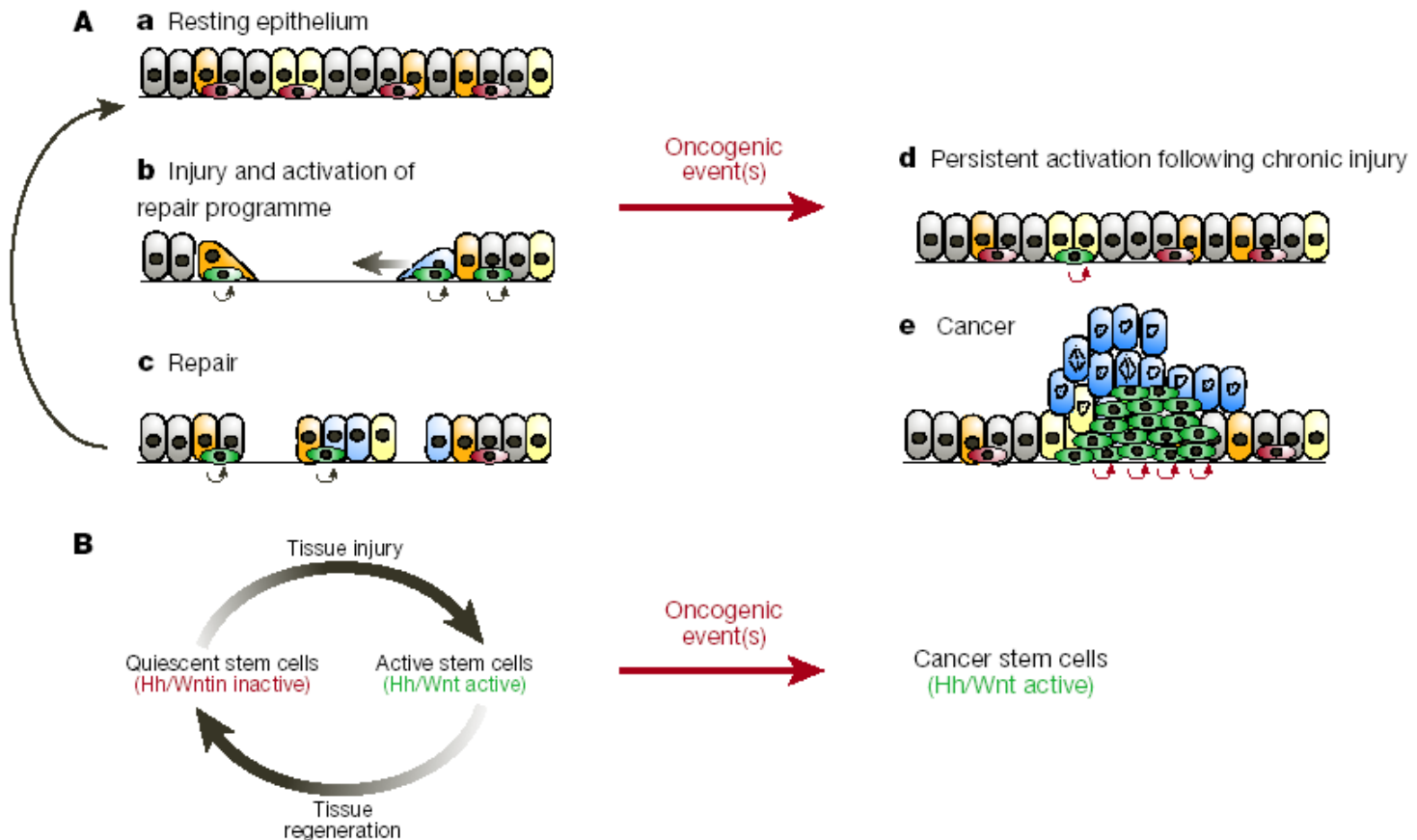


Figure 2 Model for carcinogenesis resulting from persistence of a state of injury repair.

A. Cellular events of epithelial repair. **a.** Resting epithelium with several differentiated cell phenotypes (brown, orange, and yellow) derived from tissue stem cells, now quiescent (red). Pathways such as Hh and Wnt signalling pathways that have a role in the renewal of stem cells are not active. **b.** Epithelial defect resulting from acute injury. Loss of epithelial continuity activates a repair program which is driven by Hh or Wnt signalling. This program results in the acquisition by epithelial cells of a more mesenchymal phenotype, including flattening and movement of cells (straight arrow) to cover the wound, activation (green), and expansion of stem cells through renewal divisions (curved arrows). **c.** The wound is repaired, first by rapid cell movement, and then by restoration of cell numbers resulting from the amplification of stem cells and

the differentiation of their progeny. Subsequently, either epithelial continuity and patterning is restored, Hh and Wnt signalling ceases, and the stem cell compartment returns to quiescence (**a**); or oncogenic event(s) may trap a stem cell in an activated state of continuous renewal, which is driven by autonomous Wnt or Hh signalling (**d**). Further genetic or epigenetic change in such a persistently activated stem cell (curved red arrows) might produce a cancer stem cell (green) which is capable of aggressively propagating a cancer (**e**). This may result from enhanced proliferation and production of more cancer stem cells as well as from differentiated cancer cells (blue). **B.** Stem cells cycle between quiescence and activity as a consequence of Hh/Wnt driven responses to injury. Oncogenic event(s) may trap activated stem cells in a permanent state of Hh/Wnt driven activity, resulting in cancer stem cells.

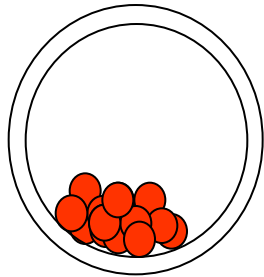
Kmenové buňky

a) sebeobnova (selfrenewal)

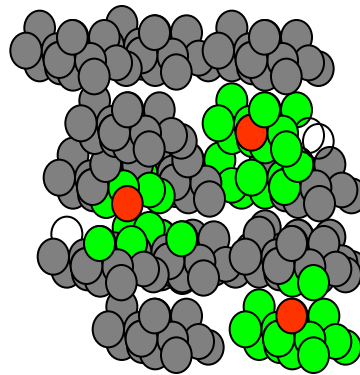
b) multipotence

- embryonální kmenové (ES)
- tkáňově specifické

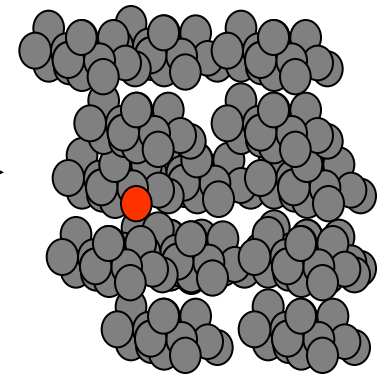
blastocysta



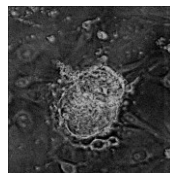
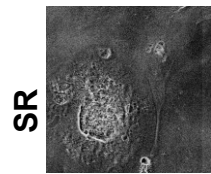
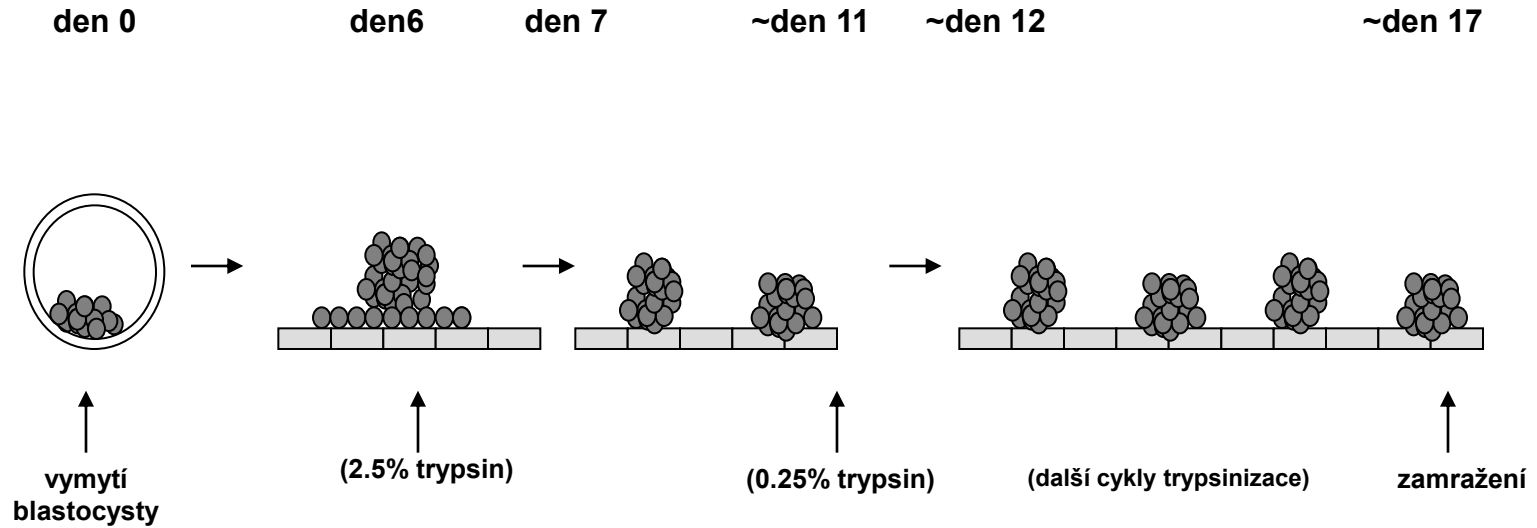
vyvíjející se tkáň (orgán)



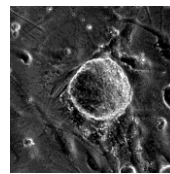
dospělá tkáň



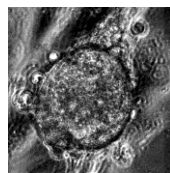
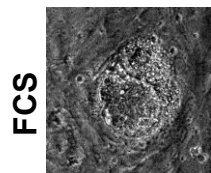
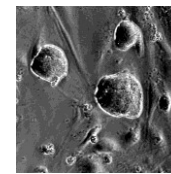
Příprava embryonálních kmenových buněk:



↓
trypsin



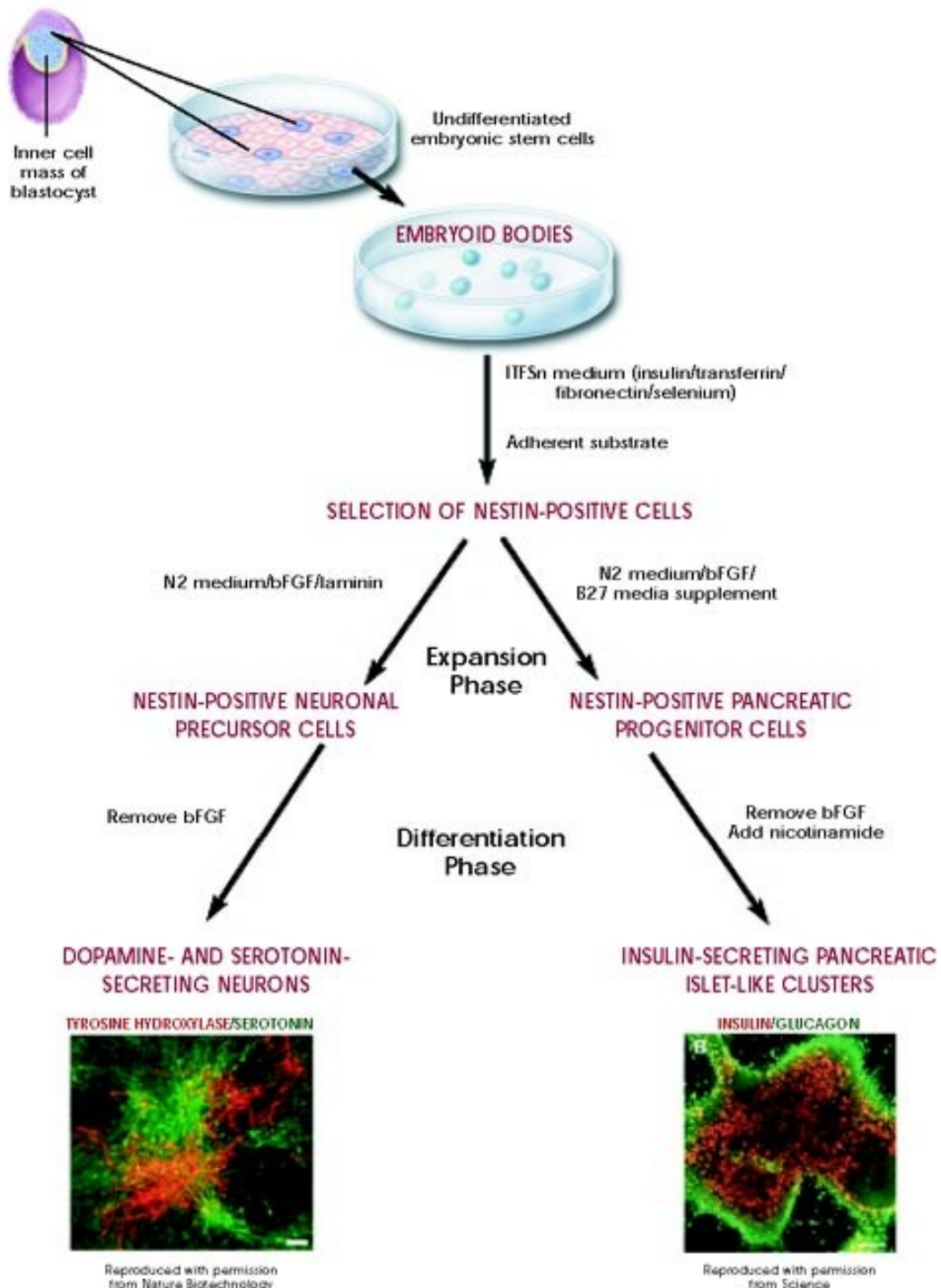
↓
trypsin



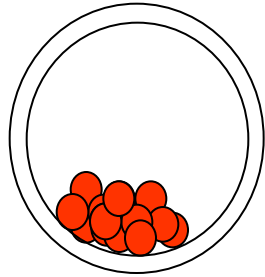
↓
trypsin

žádné kolonie
připomínající ES
buňky



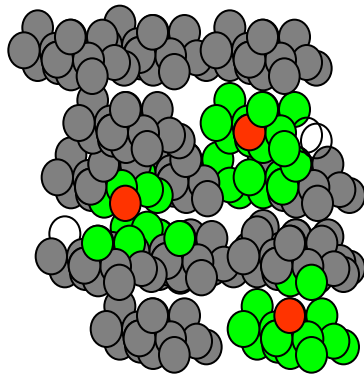


In vivo

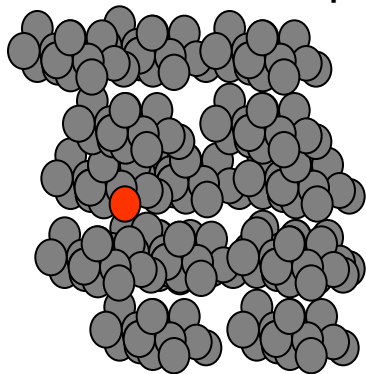


blastocysta

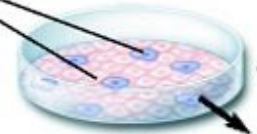
vyvíjející se tkáň (orgán)



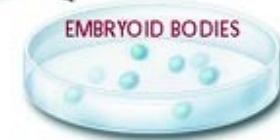
dospělá tkáň



In vitro



Undifferentiated embryonic stem cells



ITF5n medium (insulin/transferrin/
fibronectin/selenium)
Adherent substrate

SELECTION OF NESTIN-POSITIVE CELLS

N2 medium/bFGF/laminin

N2 medium/bFGF/
B27 media supplement

Expansion
Phase

NESTIN-POSITIVE NEURONAL
PRECURSOR CELLS

NESTIN-POSITIVE PANCREATIC
PROGENITOR CELLS

Differentiation
Phase

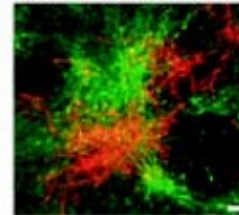
Remove bFGF

Remove bFGF
Add nicotinamide

DOPAMINE- AND SEROTONIN-
SECRETING NEURONS

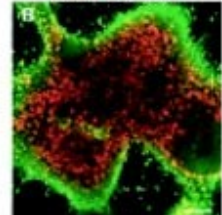
INSULIN-SECRETING PANCREATIC
ISLET-LIKE CLUSTERS

TYROSINE HYDROXYLASE/SEROTONIN



Reproduced with permission
from Nature Biotechnology

INSULIN/GLUCAGON

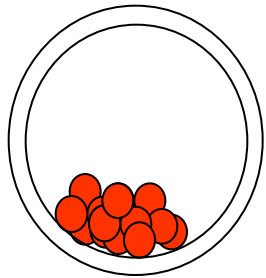


Reproduced with permission
from Science

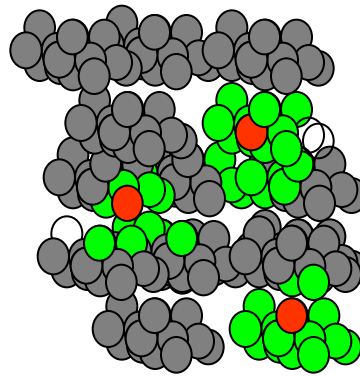
embryonální vývoj

ontogeneze

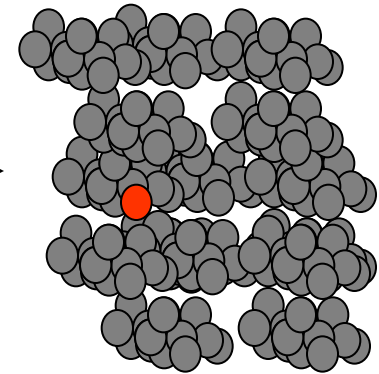
blastocysta



vyvíjející se tkáň (orgán)

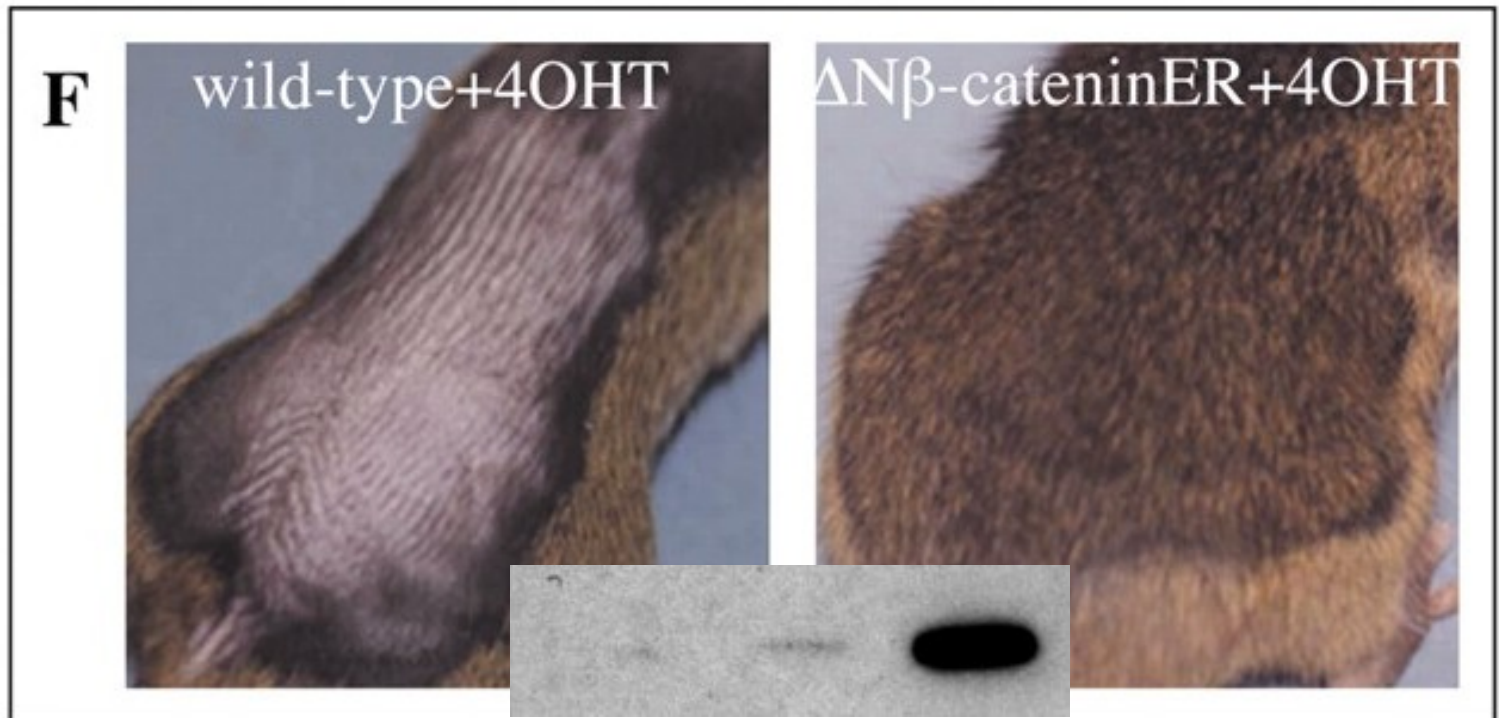


dospělá tkáň





Klíčové regulátory (Velká pětka): Wnt, Shh, BMP/TGF, RTK (FGF), Notch



Kde jsou adult stem cells a jak
vypadají?

Prostředí kmenových buněk (stem cell niche)

vlasový kořínek

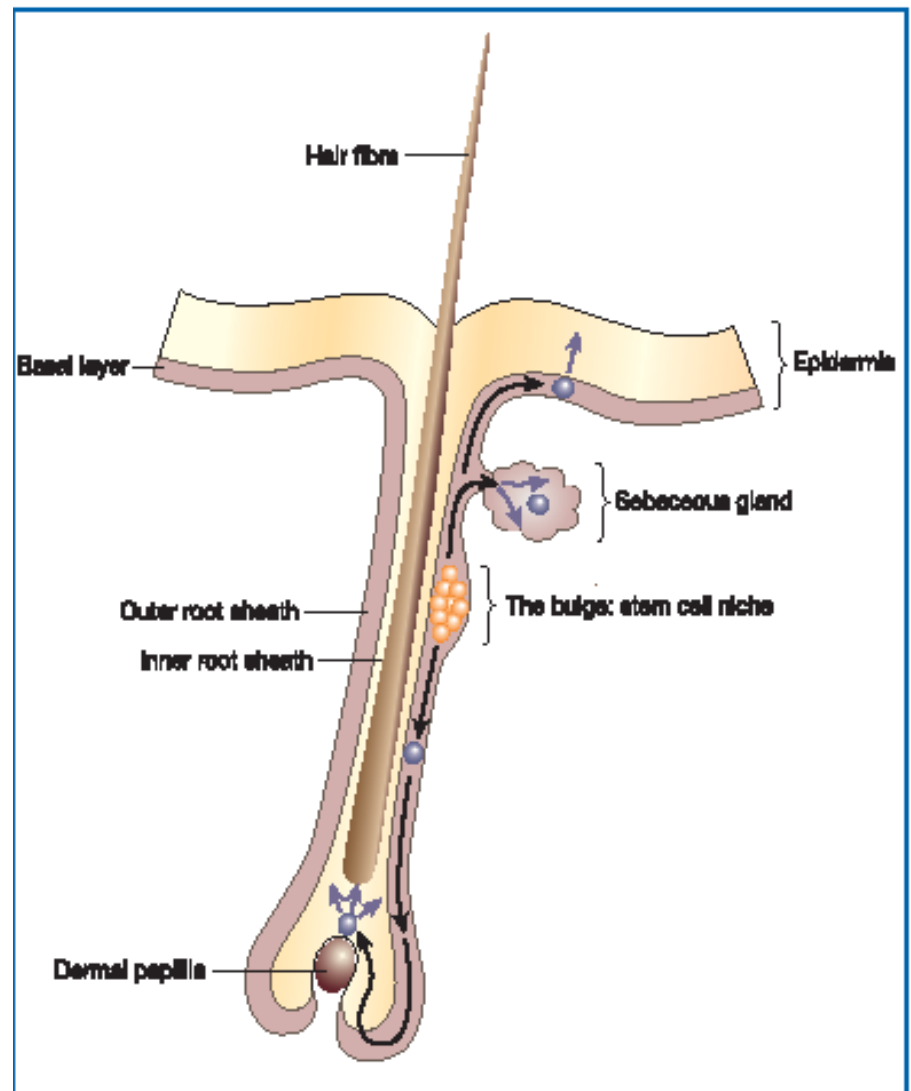
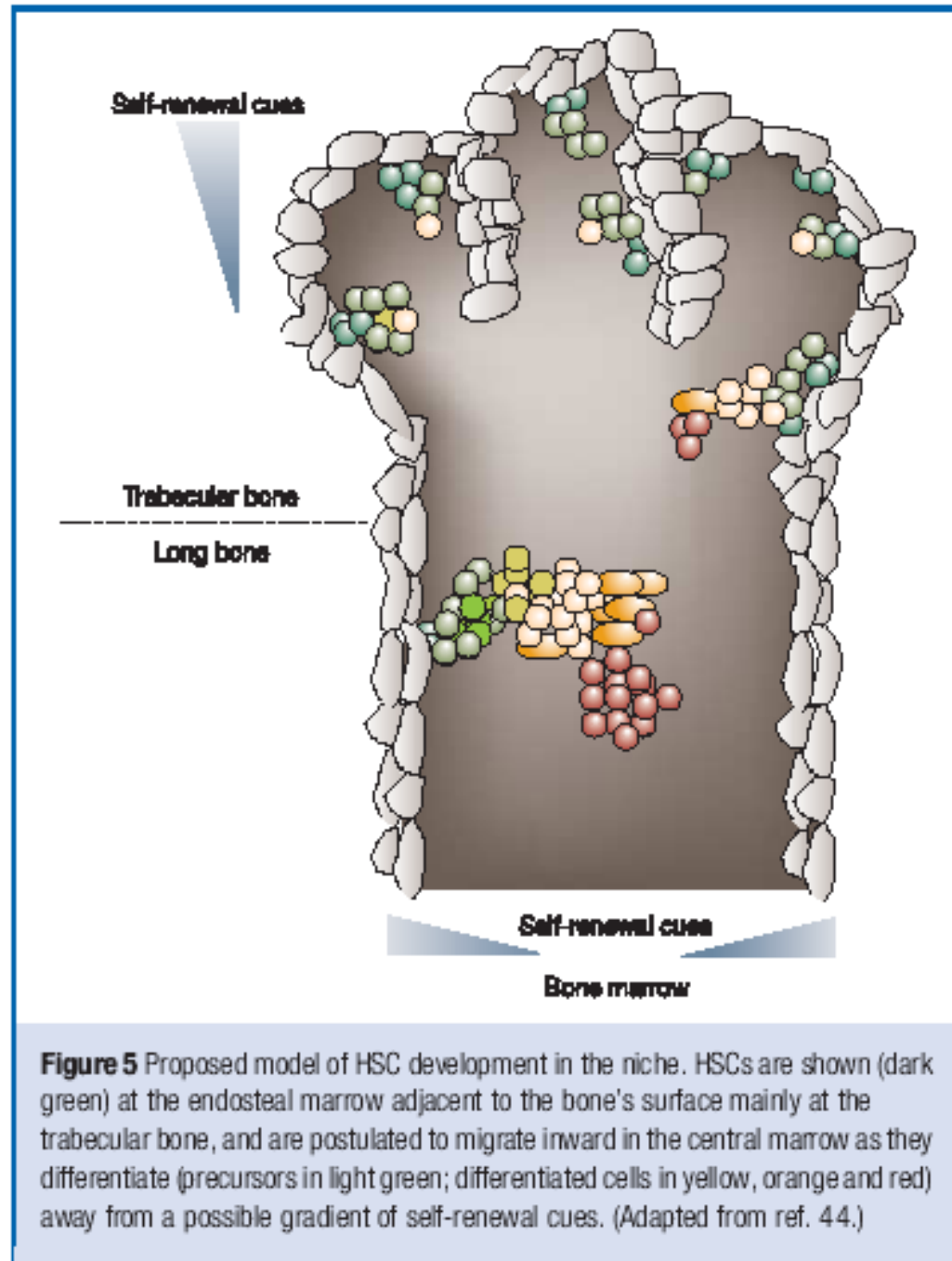


Figure 4 The hair follicle. Stem cells reside in the bulge niche. Cells can migrate upwards from here to populate the sebaceous gland and the interfollicular epidermis. Cells that migrate downwards enter the matrix where they rapidly proliferate and then differentiate to form the hair. (Adapted from ref. 90.)

Reya & Clevers 2005, Nature

Prostředí kmenových buněk (stem cell niche)

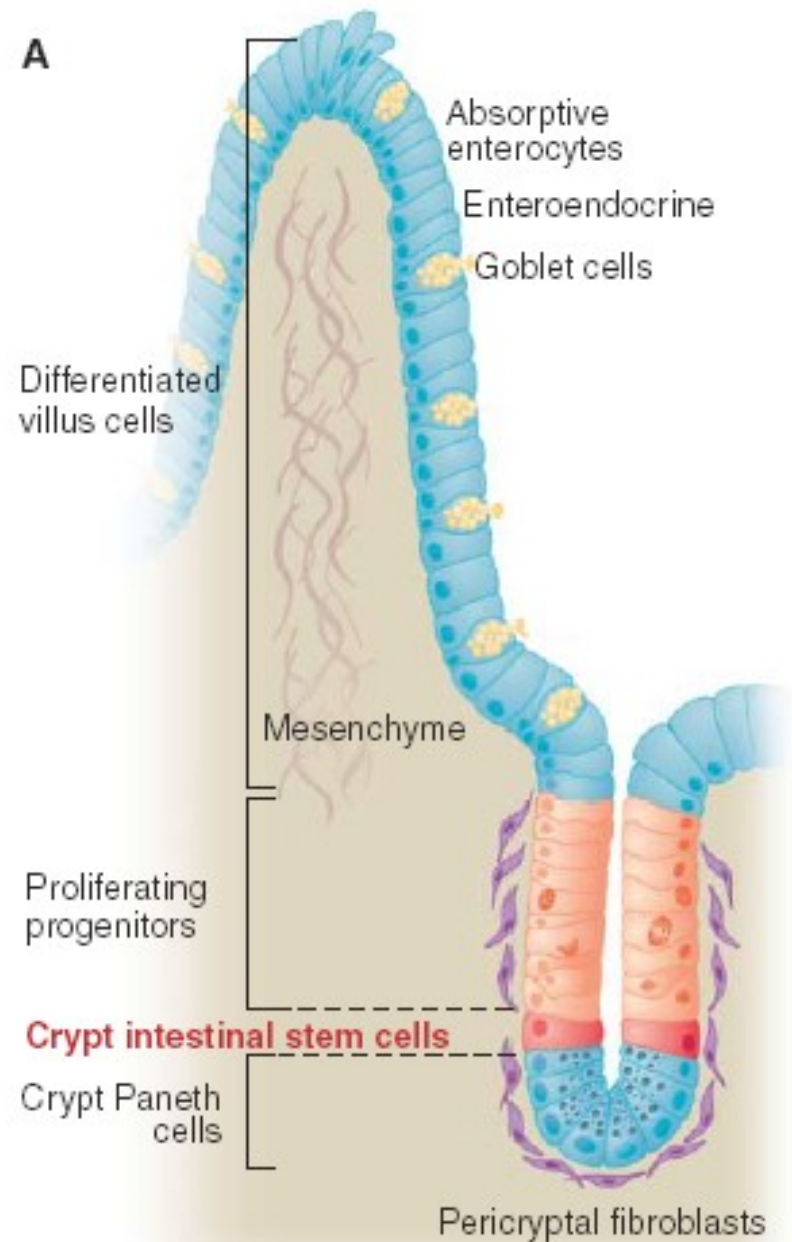
kostní dřeň



Reya & Clevers 2005, Nature

Prostředí kmenových buněk (stem cell niche)

střevní epitel

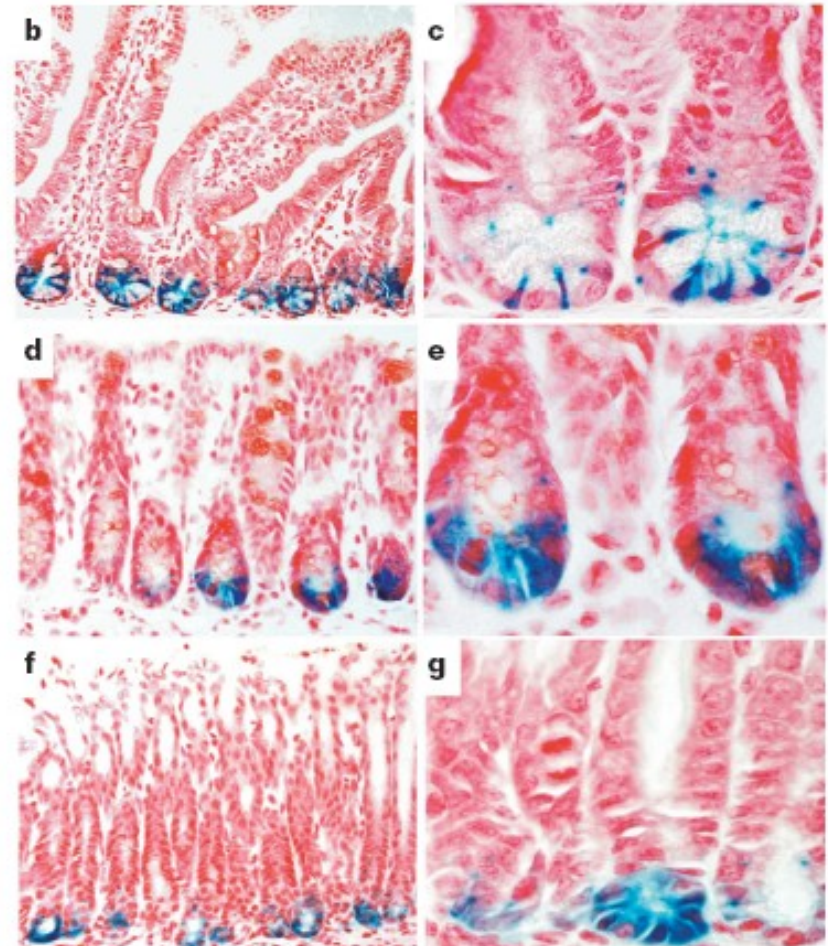
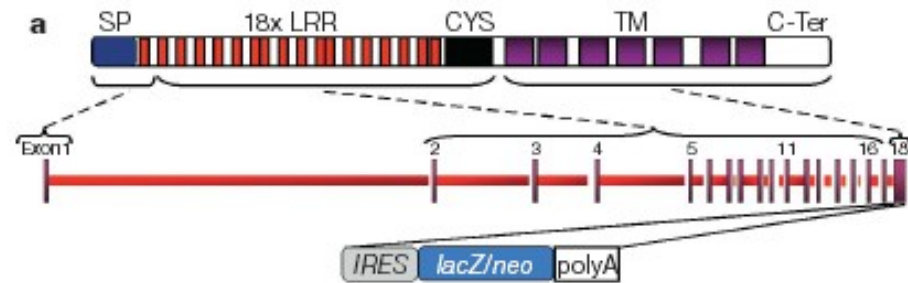


Hunt for the adult stem cells

střevní epitel – latest developments
aneb jak opravdu na to (Barker et al.,
Nature, October 2007)

A. Příprava transgenní myši č. 1 za
účelem zjistit, kde je nový potenciální
stem cell marker exprimován (in vivo
expression profiling). *Lgr5* je
exprimován specificky v buňkách ve
spodní části krypty.

Figure 3 | Restricted expression of an *Lgr5-lacZ* reporter gene in adult mice. **a**, Generation of mice carrying *lacZ* integrated into the last exon of the *Lgr5* gene, removing all transmembrane (TM) regions of the encoded *Lgr5* protein. Neo, neomycin resistance cassette; SP, signal peptide; LRR, leucine-rich repeat region; C-Ter is carboxy terminus. **b–h**, Expression of *Lgr5-LacZ* (blue) in selected adult mouse tissues. **b, c**, In the small intestine, expression is restricted to six to eight slender cells intermingled with the Paneth cells at the crypt base. **d, e**, In the colon, expression is confined to a few cells located at the crypt base. **f, g**, Expression in the stomach is limited to the base of the glands.

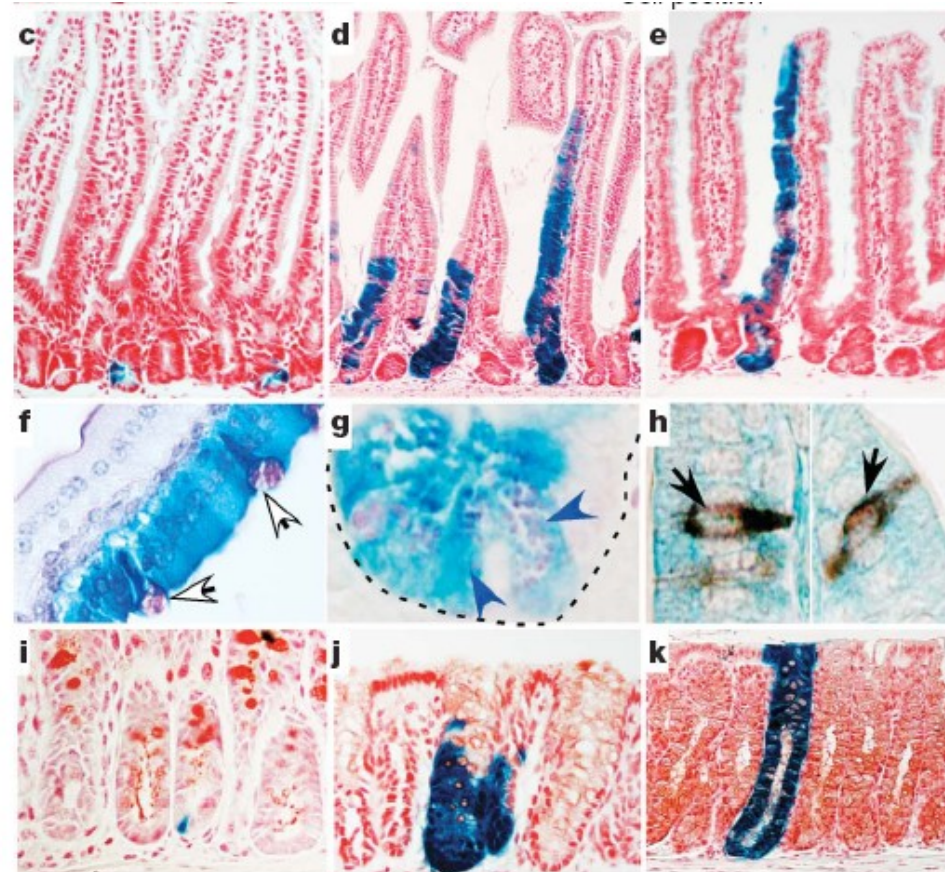
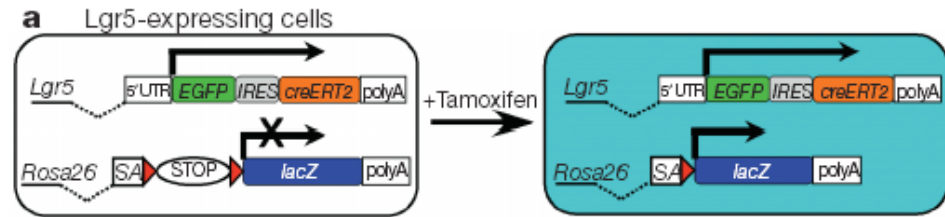


**střevní epitel – latest developments
aneb jak opravdu na to (Barker et al.,
Nature, October 2007)**

**B. Příprava transgenní myši 2, 3 a 4
za účelem zjistit, co všechno vzniká z
Lgr5-pozitivních buněk (Lgr5+
lineage tracing). Lgr5 pozitivní buňky
dávají vzniknout všem částem
buněčného epitelu.**

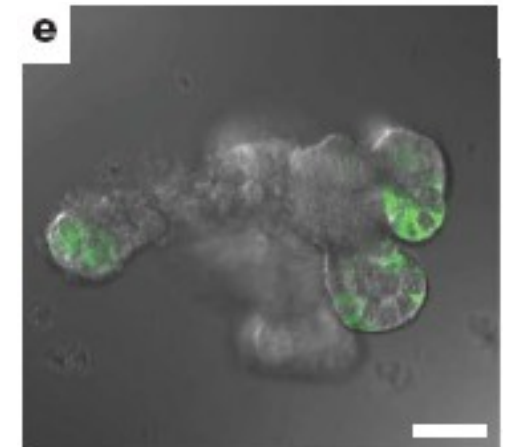
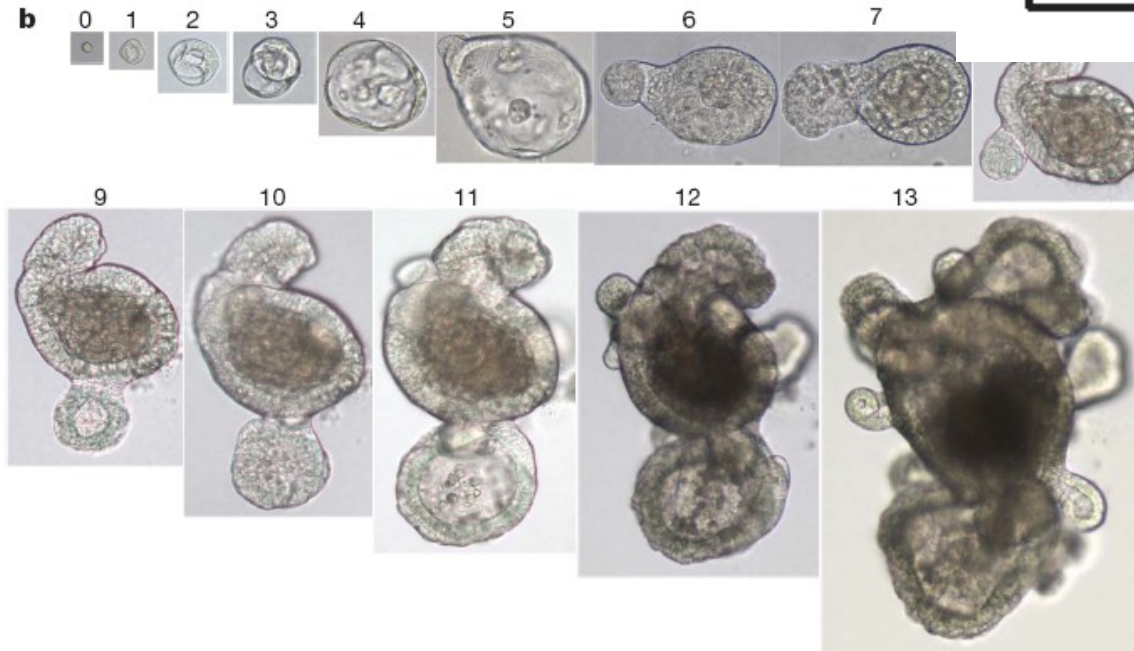
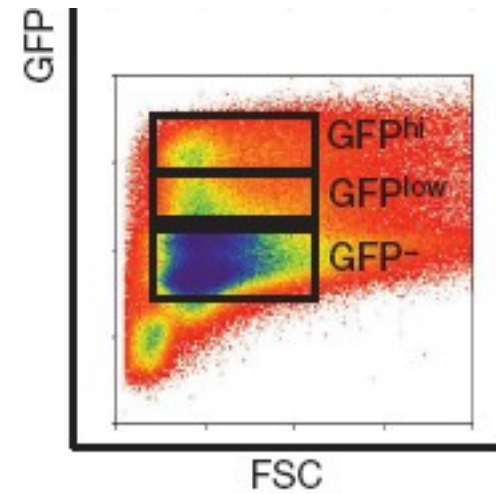
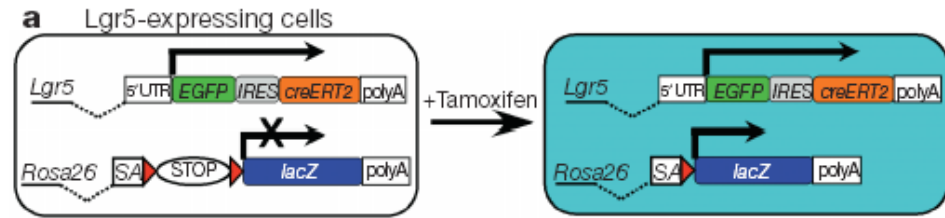
Figure 5 | Lineage tracing in the small intestine and colon. a, *Lgr5-EGFP-IRES-creERT2* knock-in mouse crossed with *Rosa26-lacZ* reporter mice 12 h after tamoxifen injection. b, Frequency at which the blue cells appeared at

carrying activated Cre. c–e, Histological analysis of LacZ activity in small intestine 1 day after induction (c), 5 days after induction (d) and 60 days after induction (e). f–h, Double-labelling of LacZ-stained intestine using PAS demonstrates the presence of goblet cells (f, white arrows) and Paneth cells (g, blue arrows) in induced blue clones. Double-labelling with synaptophysin demonstrates the presence of enteroendocrine cells within the induced blue clones (h, black arrows). i–k, Histological analysis of LacZ activity in colon 1 day after induction (i), 5 days after induction (j) and 60 days after induction (k).



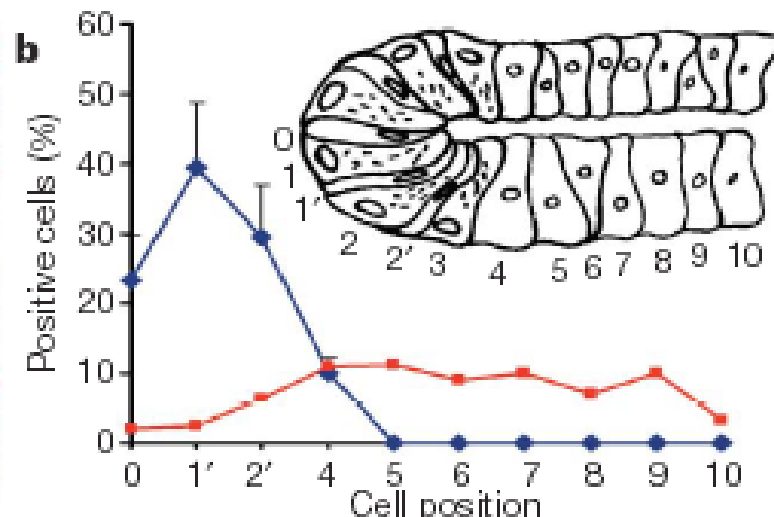
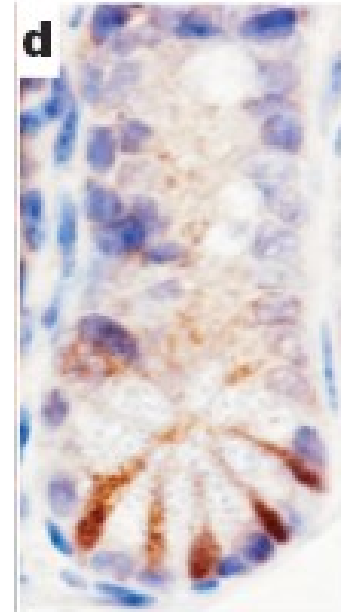
**střevní epitel – latest developments
aneb jak opravdu na to (Barker et al.,
Nature & Sato, Nature 2009)**

**C. Lgr5 pozitivní buňky in vitro dávají
vzniknout kompletní villus-crypt
strukturu in vitro (Doposud se to s
žádnými jinými buňkami nepodařilo)**



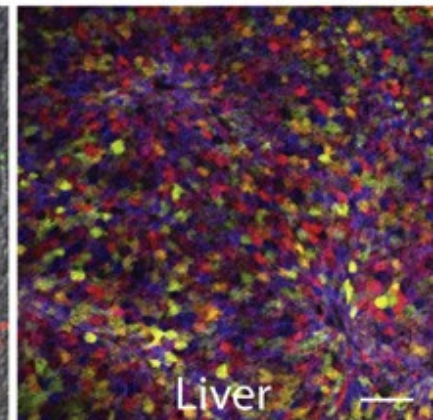
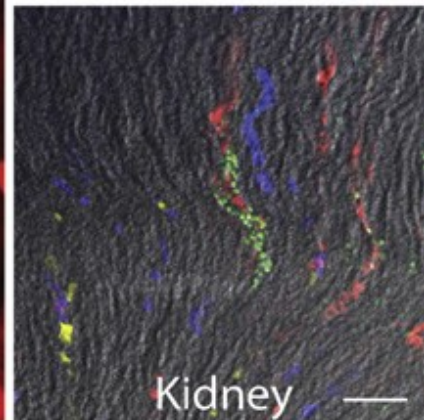
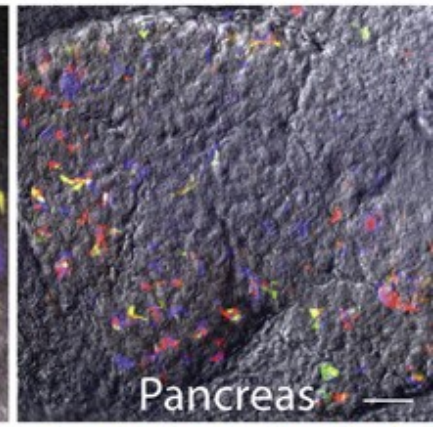
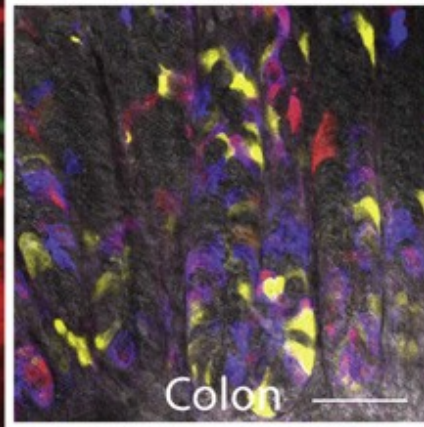
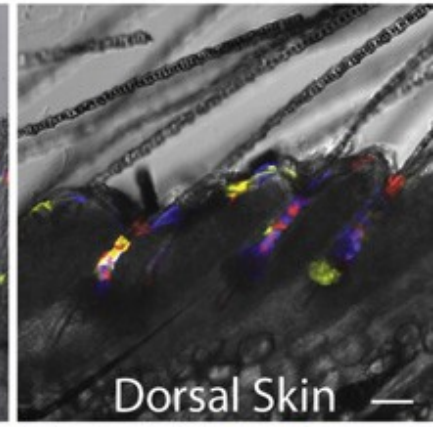
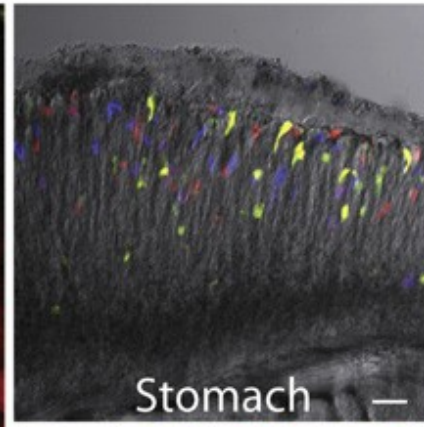
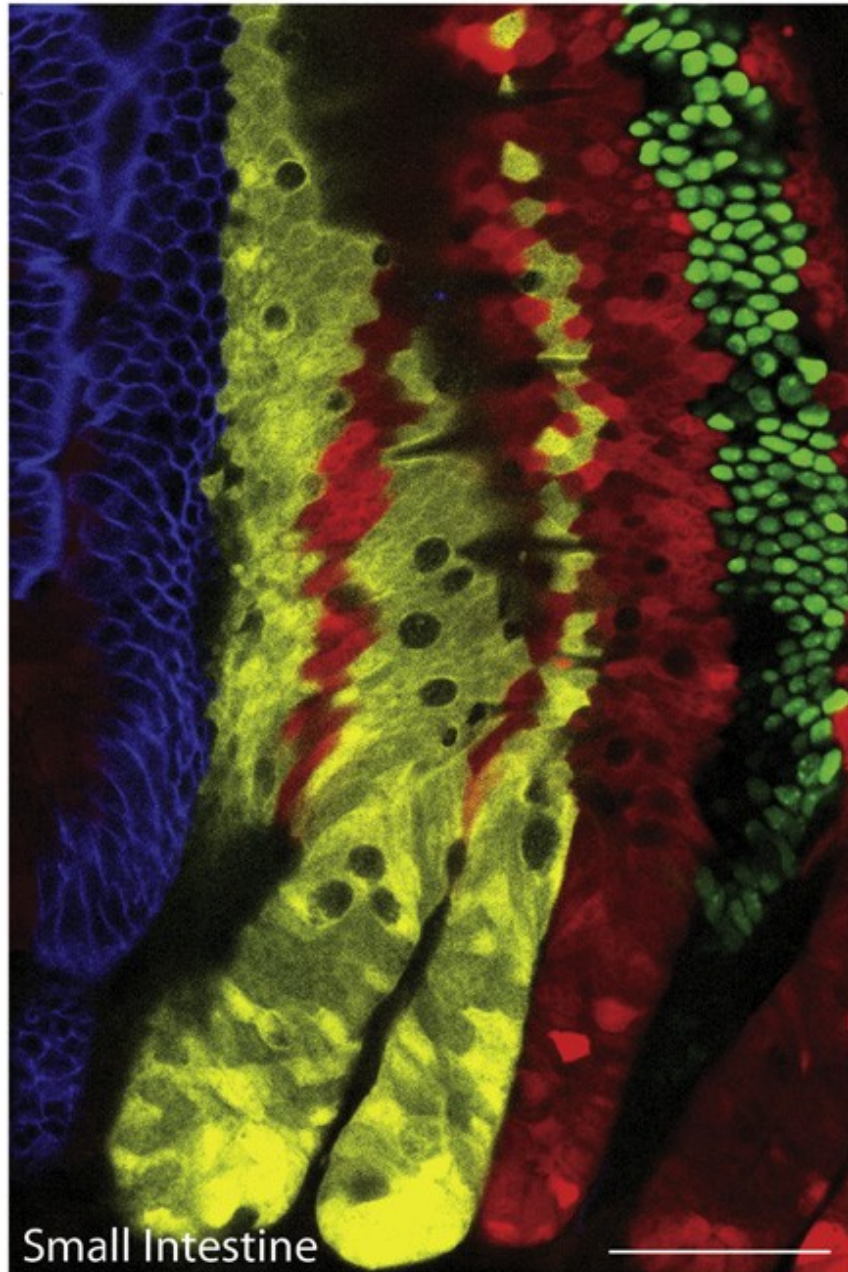
**střevní epitel – latest developments
aneb jak opravdu na to (Barker et al.,
Nature, October 2007)**

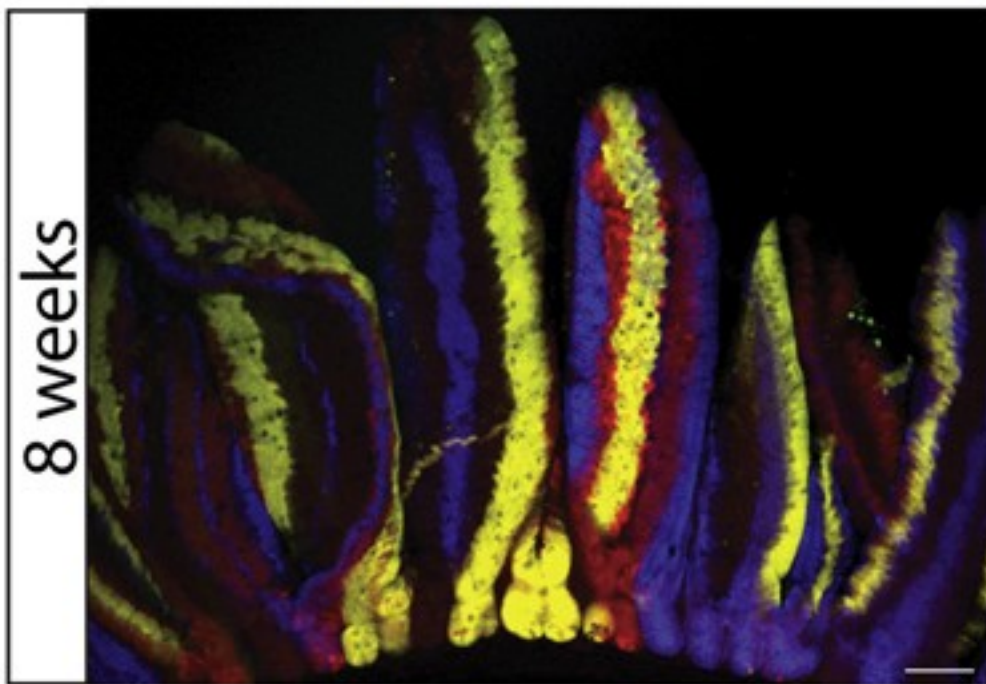
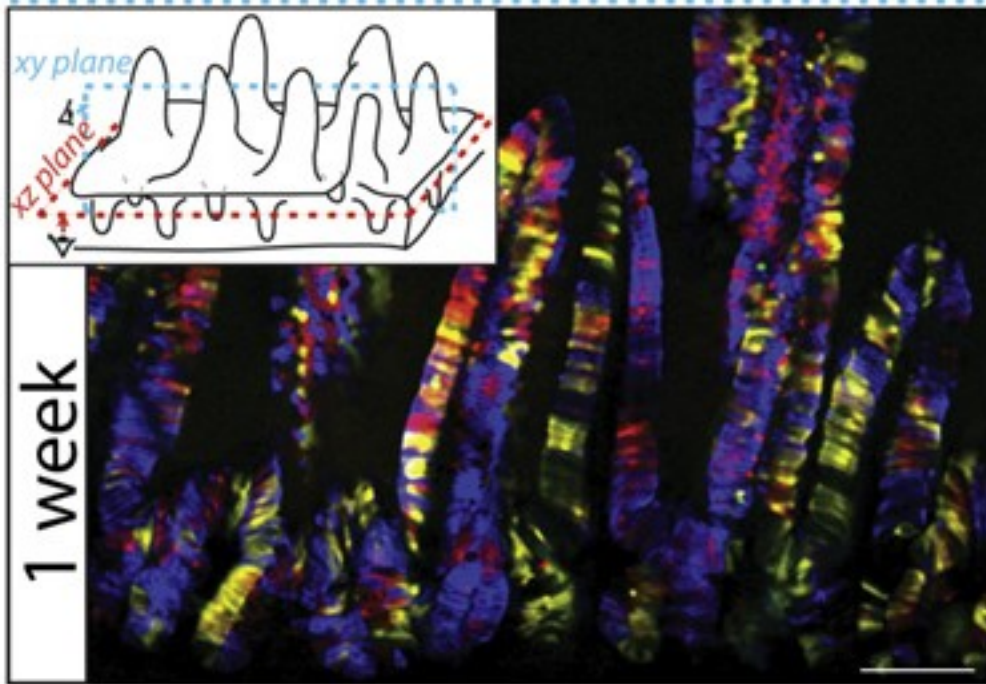
**D. Závěr: Kmenové buňky epitelu
tlustého i tenkého střeva jsou
protáhlé, dříve nepovšimnuté buňky,
v relativní pozici 1', 2' a 3' od spodu
krypty.**



Rosa26 locus in Mouse, Chr6

Cre recombination





Cell

Intestinal Crypt Homeostasis Results from Neutral Competition between Symmetrically Dividing Lgr5 Stem Cells

Hugo J. Snippert,¹ Laurens G. van der Flier,¹ Toshiro Sato,¹ Johan H. van Es,¹ Maaïke van den Born,¹ Carla Kroon-Veenboer,¹ Nick Barker,¹ Allon M. Klein,^{2,3} Jacco van Rheenen,¹ Benjamin D. Simons,³ and Hans Clevers^{1,*}

¹Hubrecht Institute, KNAW and University Medical Center Utrecht, Uppsalalaan 8, 3584 CT Utrecht, The Netherlands

²Department of Systems Biology, Harvard Medical School, 200 Longwood Avenue, Boston, MA 02115, USA

³Department of Physics, Cavendish Laboratory, J.J. Thomson Avenue, Cambridge CB3 0HE, UK

*Correspondence: h.clevers@hubrecht.eu

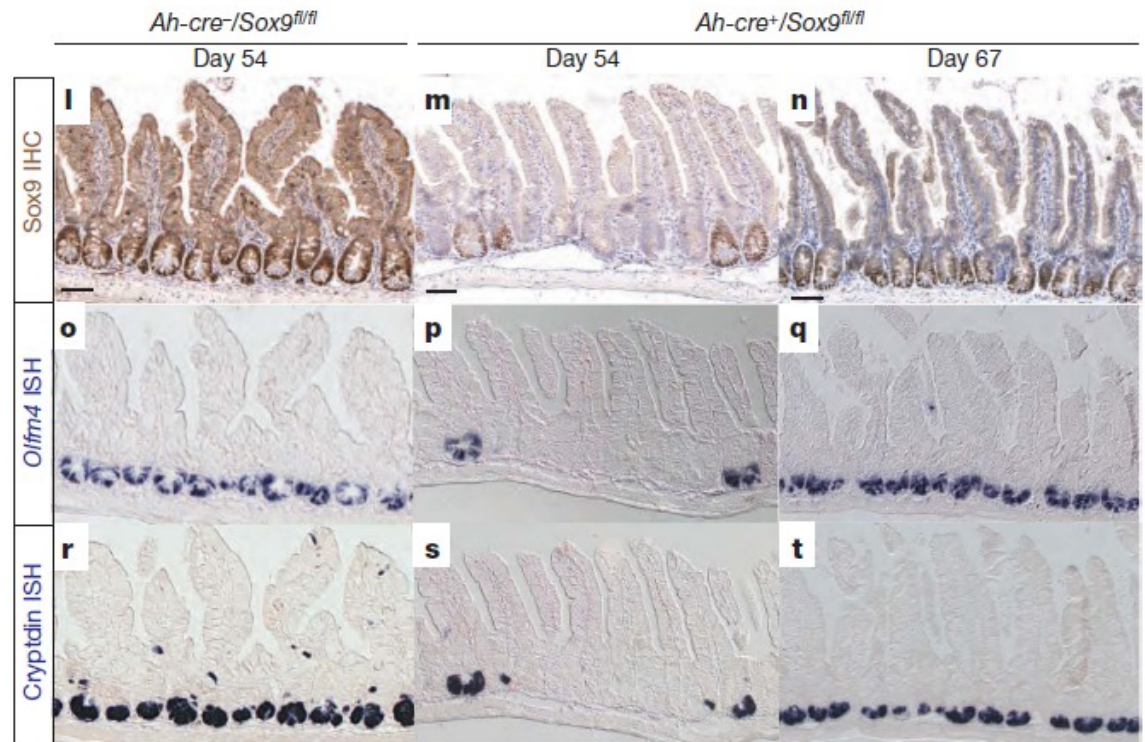
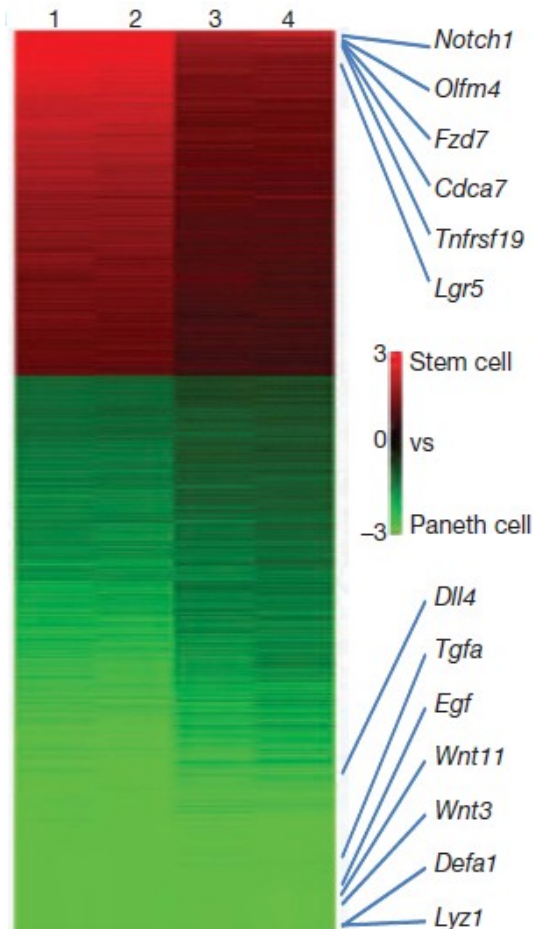
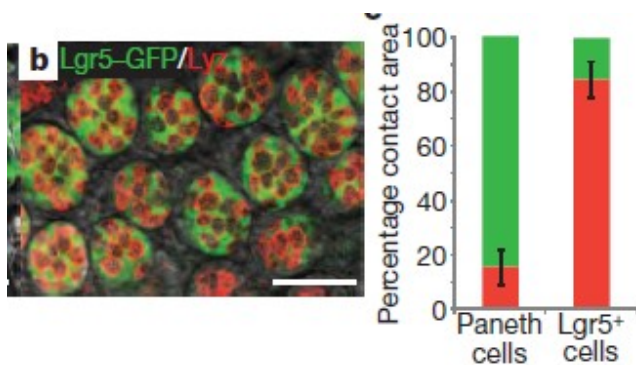
DOI 10.1016/j.cell.2010.09.016

Paneth cells constitute the niche for Lgr5 stem cells in intestinal crypts

Toshiro Sato¹, Johan H. van Es¹, Hugo J. Snippert¹, Daniel E. Stange¹, Robert G. Vries¹, Maaïke van den Born¹, Nick Barker¹, Noah F. Shroyer², Marc van de Wetering¹ & Hans Clevers¹

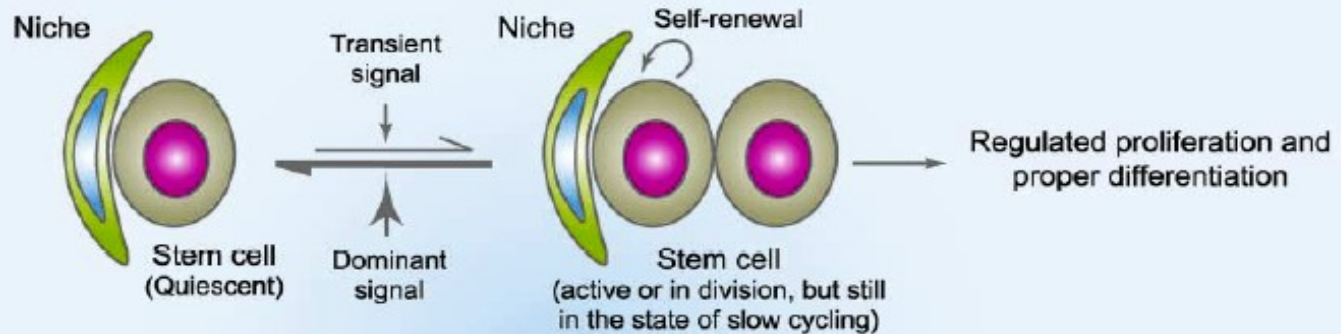
¹Hubrecht Institute, KNAW and University Medical Center Utrecht, Uppsalalaan 8, 3584CT Utrecht, the Netherlands. ²Cincinnati Children's Hospital, Division of Gastroenterology, Medical Center, MLC 2010, 3333 Burnet Avenue, Cincinnati, Ohio 45229, USA.

20 JANUARY 2011 | VOL 469 | NATURE | 415

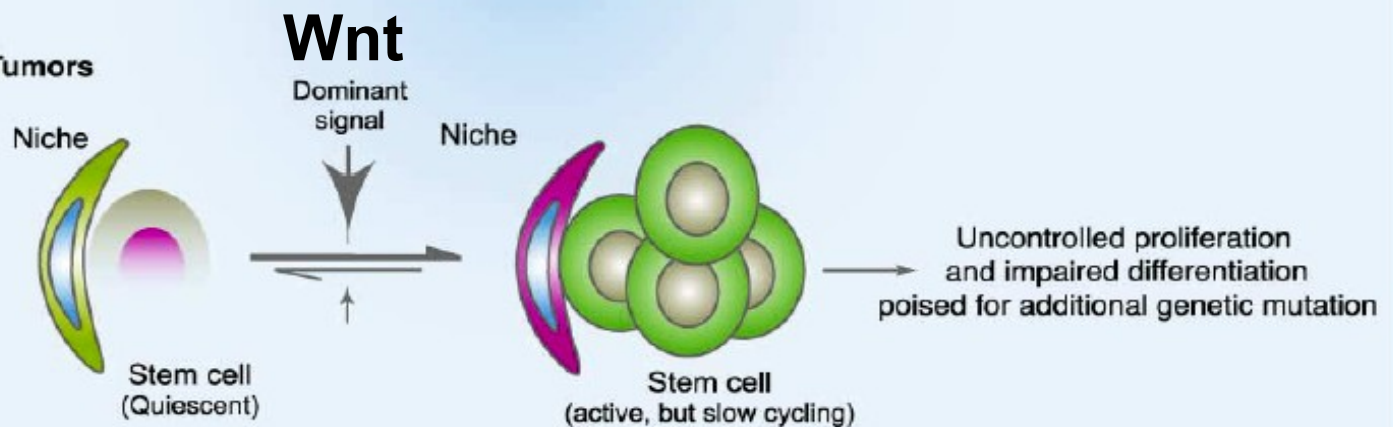


Prostředí kmenových buněk (stem cell niche)

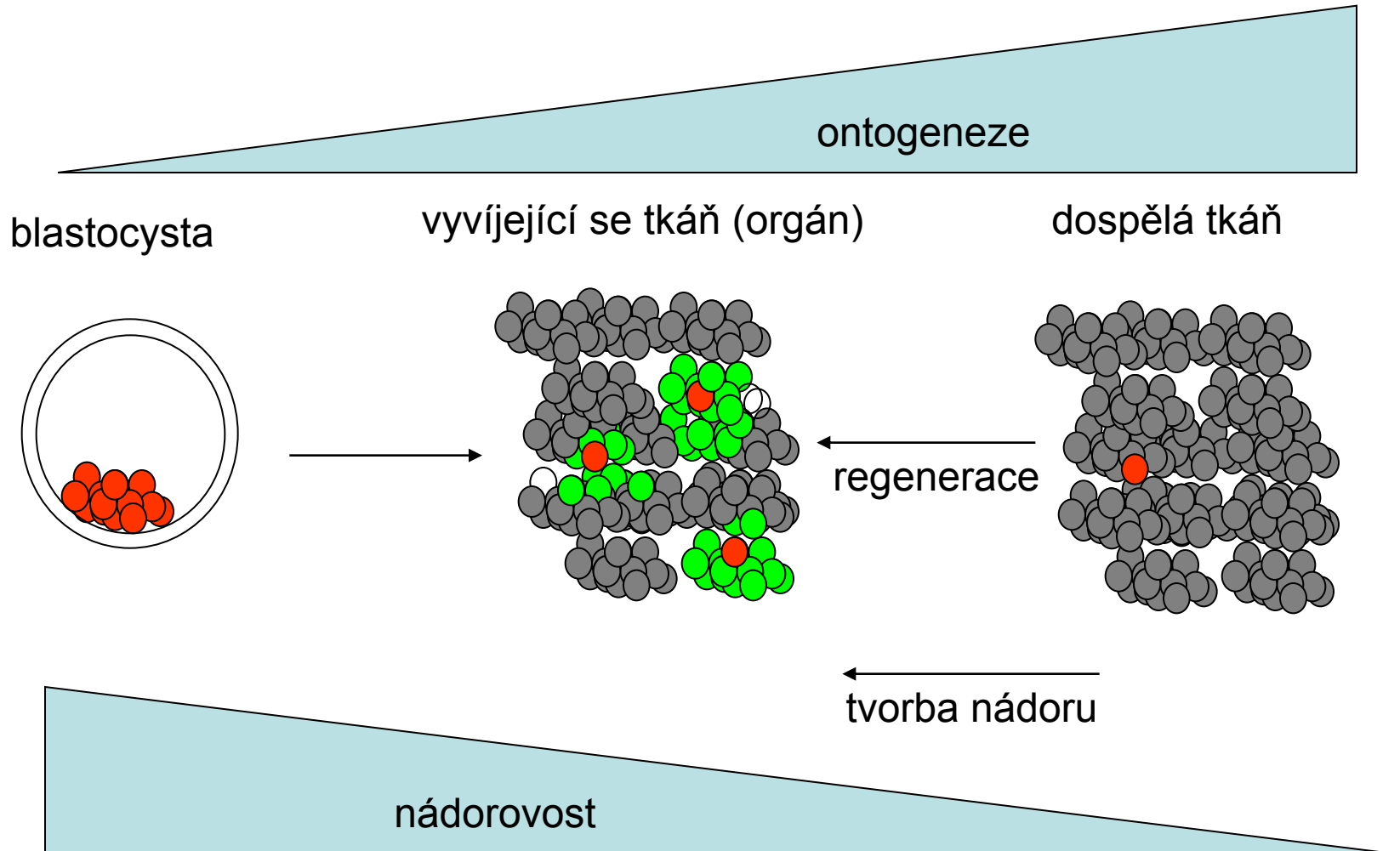
Under Normal Physiological Conditions



In Cancers or Tumors



Cancer stem cell hypothesis



Klasické morfogenetické dráhy (Wnt, Hh, Notch a další) regulují regeneraci, tkáňové specifické kmenové buňky i nádory

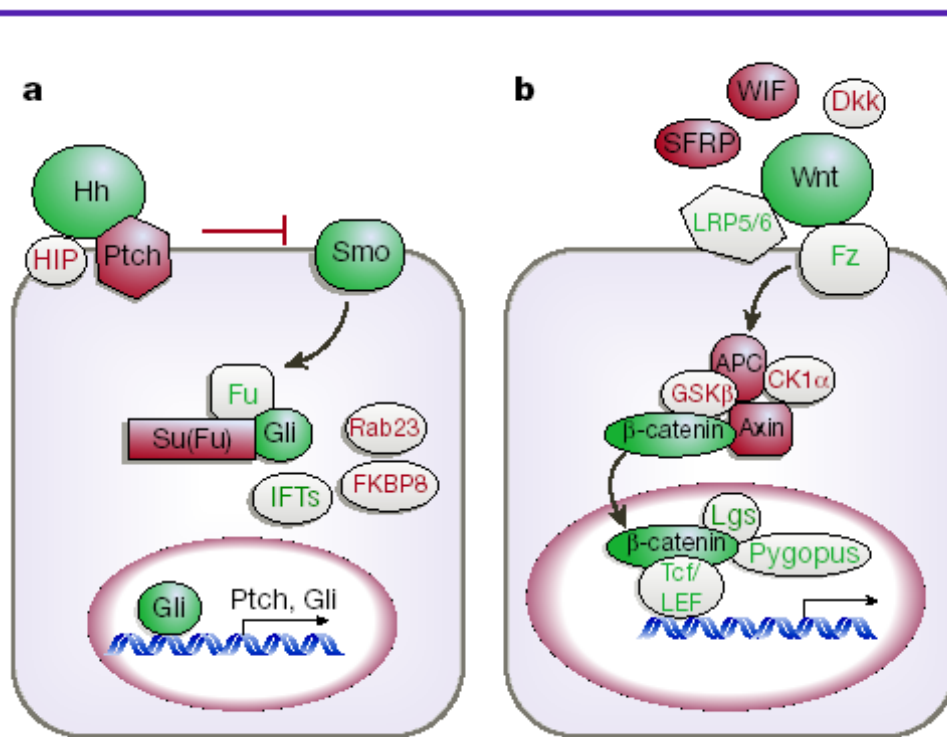
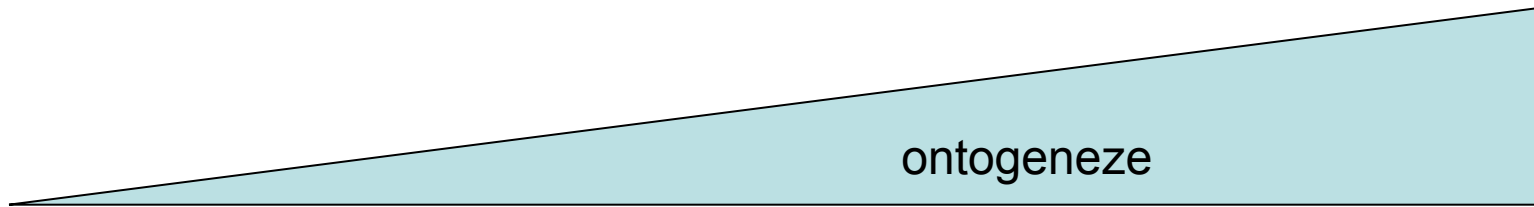


Figure 1 Hh and Wnt signalling pathways. Simplified views of the Hh and Wnt signalling pathways, with emphasis on components implicated in cancer or tissue regeneration. Green and red colours denote pathway components with primarily positive or negative roles, respectively, in pathway activation. Shaded components have been causally implicated in tumorigenesis (see Table 2 and text; more complete pathway descriptions are available in refs 32–34 for Hh and refs 17, 46 for Wnt). **a**, Activation of the Hh signalling pathway is initiated by binding of a Hh ligand to Ptch. This lifts suppression of Smo, activating a cascade that leads to the nuclear translocation of Gli and the activation of target genes. HIP is a membrane protein that antagonizes pathway activity by binding to Hh ligands, and Fu, Su(Fu), Rab23, FKBP8 and the IFTs (intraflagellar transport proteins) act downstream of Ptch and Smo to regulate Gli. The function of Rab23, FKBP8 and the IFTs outside the CNS is not established. HIP, Hh-interacting protein; Rab23, a member of the Rab family of GTPases; FKBP8, a member of the FK506-binding protein family. **b**, The Wnt signalling pathway is activated by binding of Wnt ligands to their receptors Fz and LRP5/6, leading to the release of β -catenin from the degradation complex and facilitating its entry into the nucleus, where it regulates target gene transcription through association with Tcf/LEF, Legless (Lgs) and Pygopus. SFRP, Wnt inhibitory factor; Dkk, Dickkopf; GSK3 β , glycogen synthase kinase 3 β ; CK1a, casein kinase 1a.

Table 2 **Hh and Wnt pathways in cancer**

Tissue	Tumour	Evidence of pathway involvement	References
Hh pathway			
Brain	Medulloblastoma	Tumorigenesis by inactivation of <i>PTCH</i> ; allograft and cell-line growth inhibition by cyclopamine; inhibition of autochthonous tumour growth by synthetic small molecule antagonist	37, 81; reviewed in 6
		Tumorigenesis by inactivation of <i>Su(fu)</i>	86
	Glioma	<i>Gli</i> amplification; growth inhibition of some cell lines by cyclopamine	87, 88
Skin	Basal cell carcinoma	Tumorigenesis by inactivation of <i>PTCH</i> ; <i>in vivo</i> tumorigenesis by expression of activating form of <i>SMO</i> or by <i>Shh</i> overexpression and <i>in vitro</i> growth inhibition by synthetic Hh pathway antagonist; inhibition of human tumour growth topical cyclopamine	82, 83; reviewed in 6
Muscle	Rhabdomyosarcoma	Tumorigenesis by inactivation of <i>PTCH</i>	reviewed in 6
Oesophagus	Adenocarcinoma	Cell-line growth inhibition by cyclopamine, Hh blocking antibody	42
Stomach	Adenocarcinoma	Cell-line growth inhibition by cyclopamine, Hh blocking antibody	42
Pancreas	Adenocarcinoma	Xenograft and cell-line growth inhibition by cyclopamine, Hh blocking antibody; tumour initiation (in mouse) by <i>Shh</i> overexpression	42, 43
Biliary tract	Adenocarcinoma	Xenograft and cell-line growth inhibition by cyclopamine, Hh blocking antibody	42
Lung	Small-cell lung cancer	Xenograft and cell-line growth inhibition by cyclopamine, Hh blocking antibody	41
Prostate	Adenocarcinoma	Xenograft and cell-line growth inhibition and suppression of metastasis by cyclopamine; increased xenograft growth by <i>Shh</i> and <i>Gli</i> overexpression	29, 89, 90
Bladder	Urothelial carcinoma	Increased tumour induction (in mouse) by alkylating agent in <i>Ptch</i> heterozygote	91
Oral cavity	Squamous cell cancer	Growth inhibition of cell lines by cyclopamine;	92
Wnt pathway			
Colon	Adenocarcinoma	Tumorigenesis by inactivation of APC, Axin; tumorigenesis by stabilization of β -catenin; epigenetic inactivation of SFRPs	47; reviewed in 45
Liver	Hepatoblastoma	Tumorigenesis (in mouse) by inactivation of APC and by stabilization of β -catenin	reviewed in 45
Blood	Multiple myeloma	Cell-growth inhibition by dominant negative TCF4; growth stimulation by Wnt ligand	93
Hair follicle	Pilomatricoma	Tumorigenesis (in mouse) by overexpression of β -catenin	reviewed in 45
Bone	Osteosarcoma	<i>Dkk3</i> and <i>LRP5</i> expression inhibits tumour cell growth <i>in vitro</i>	94, 95
Lung	Non-small-cell carcinoma	Apoptosis and cell-growth inhibition by short interfering RNA and a blocking antibody against Wnt2	96
Pleura	Mesothelioma	Apoptosis and cell-growth inhibition by transfection of SFRP	97

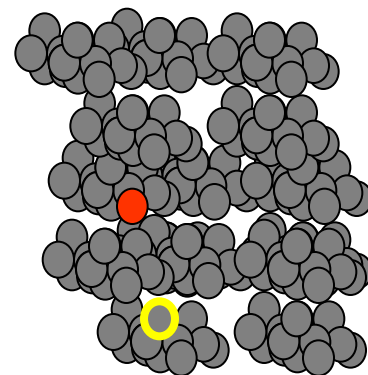
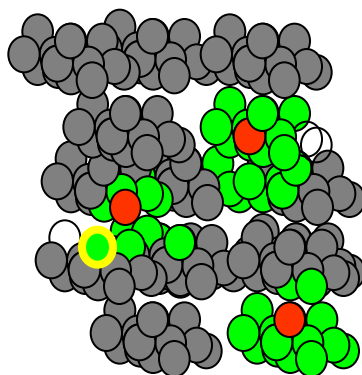
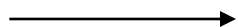
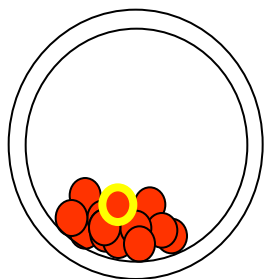
Emphasis is placed on functional data showing a requirement for pathway activation in tumour formation and/or tumour cell growth. (See Fig. 1 and text for gene abbreviations.)



blastocysta

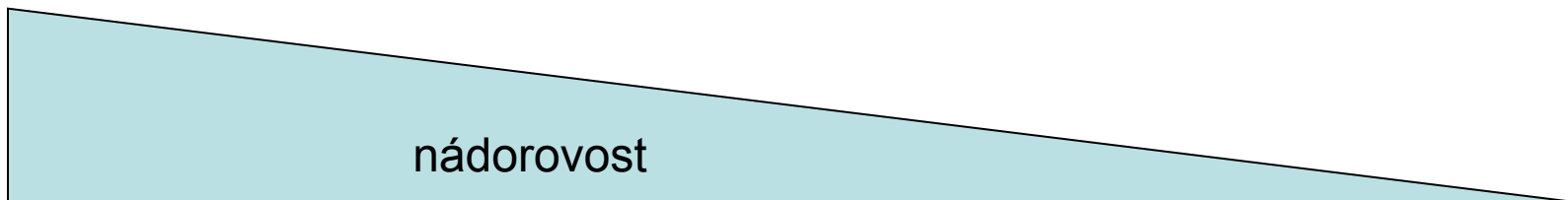
vyvíjející se tkáň (orgán)

dospělá tkáň

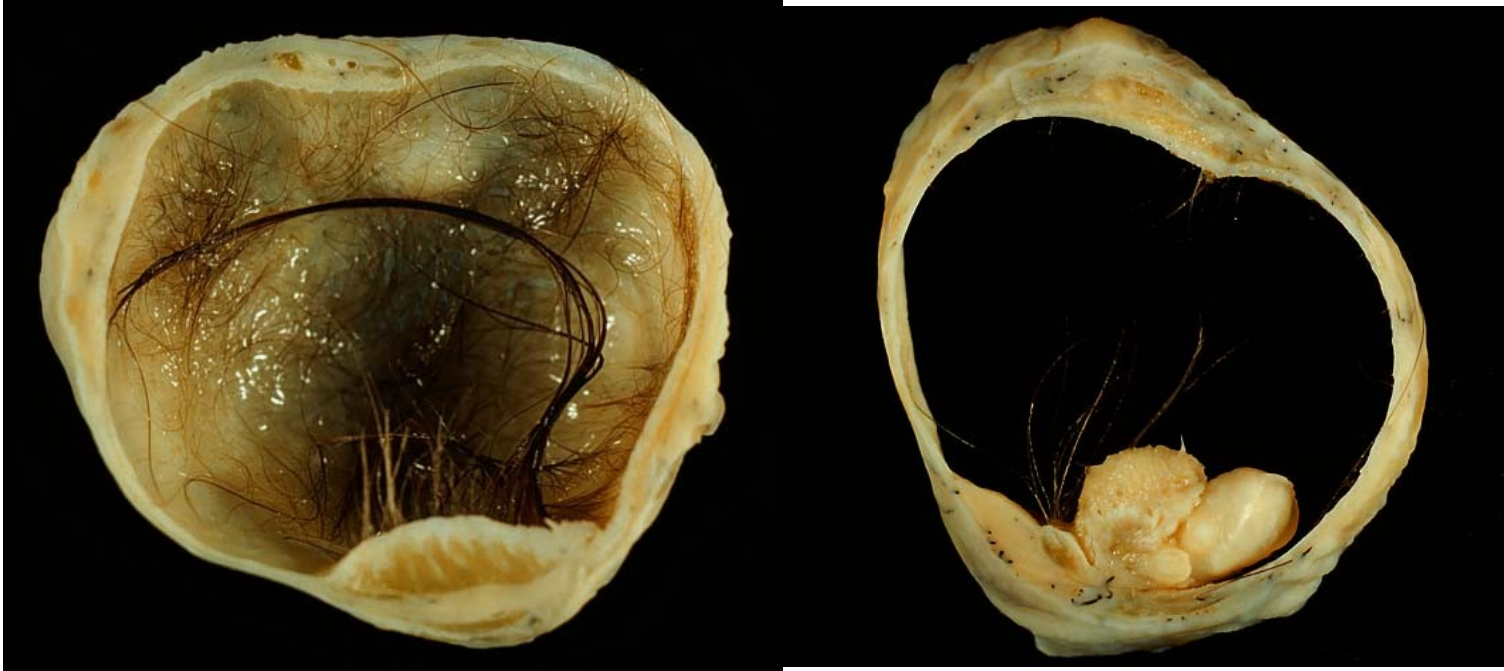


Počet mutací nutných
pro vznik nádoru:

0



Teratoma

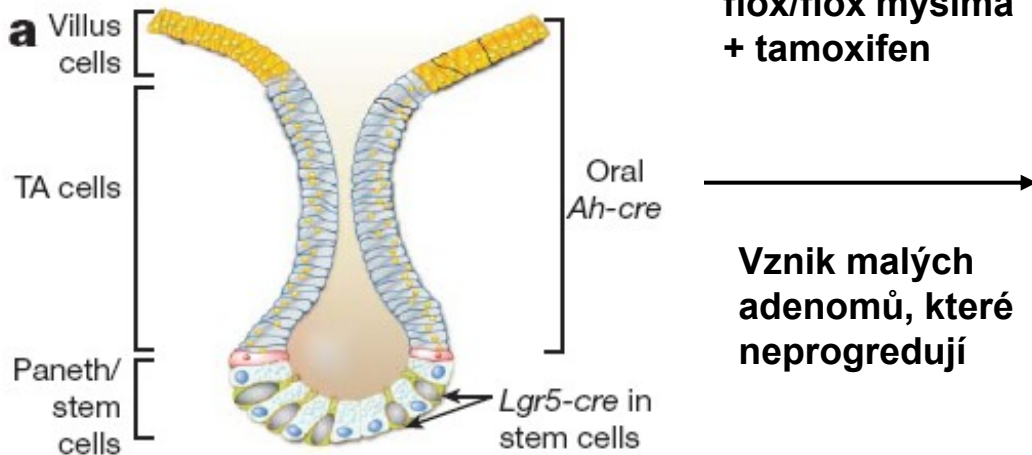


Je to pravda?

Počet
pro v

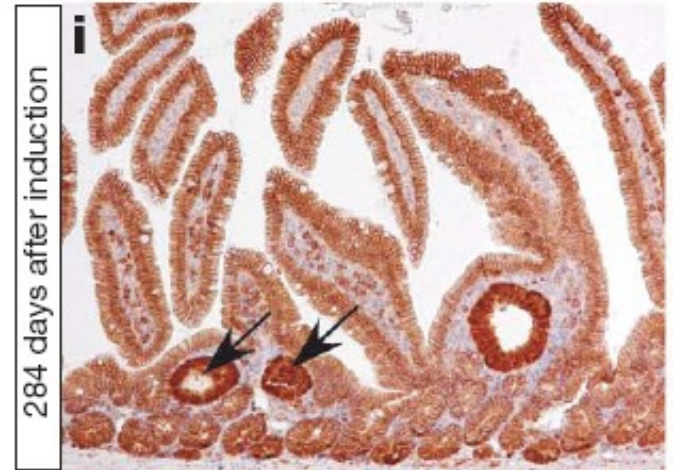
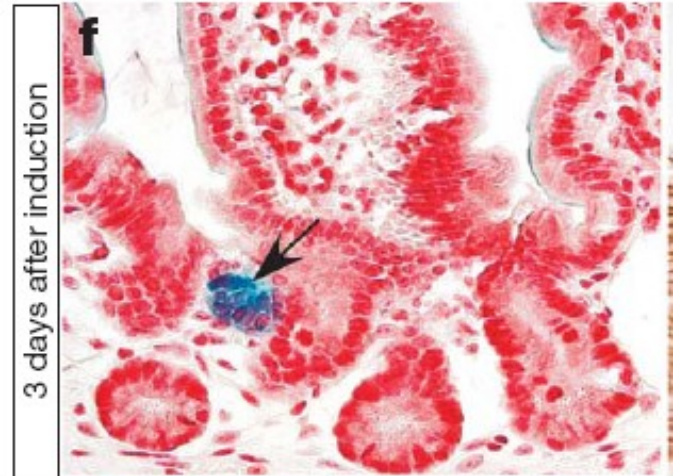
nádorovost

Experimentální důkaz:

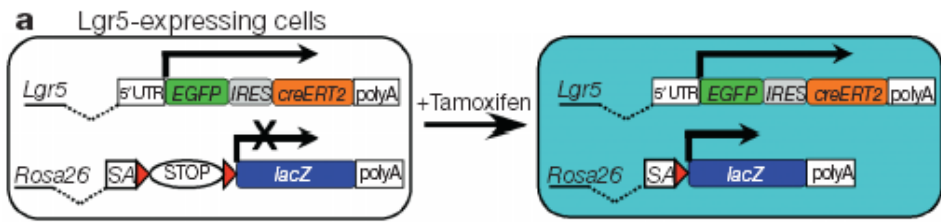


Zkřížení s APC flox/flox myšima + tamoxifen

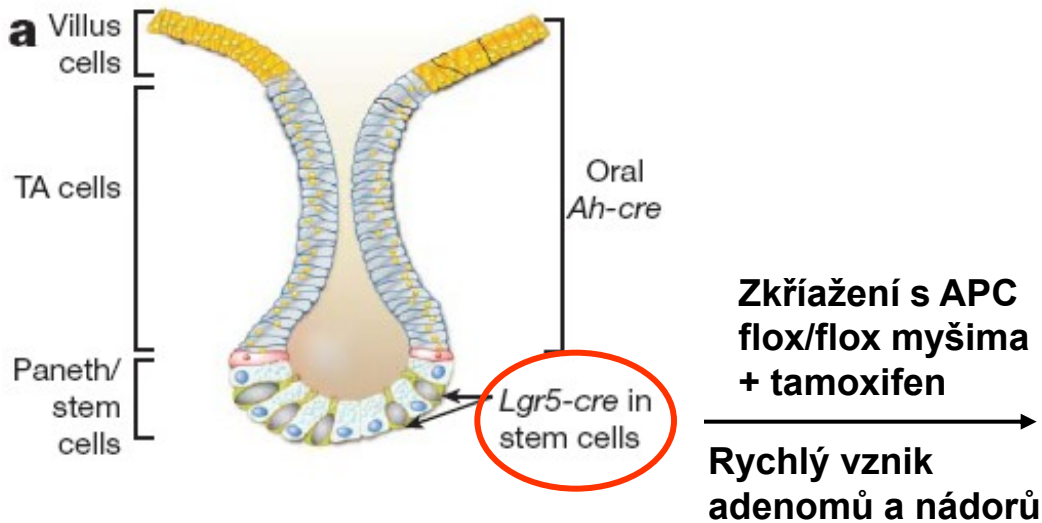
Vznik malých adenomů, které neprogredují



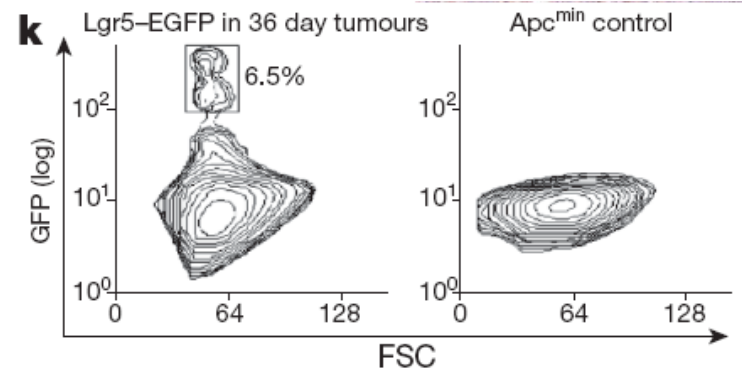
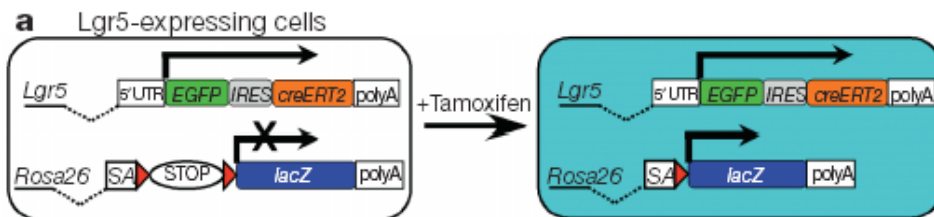
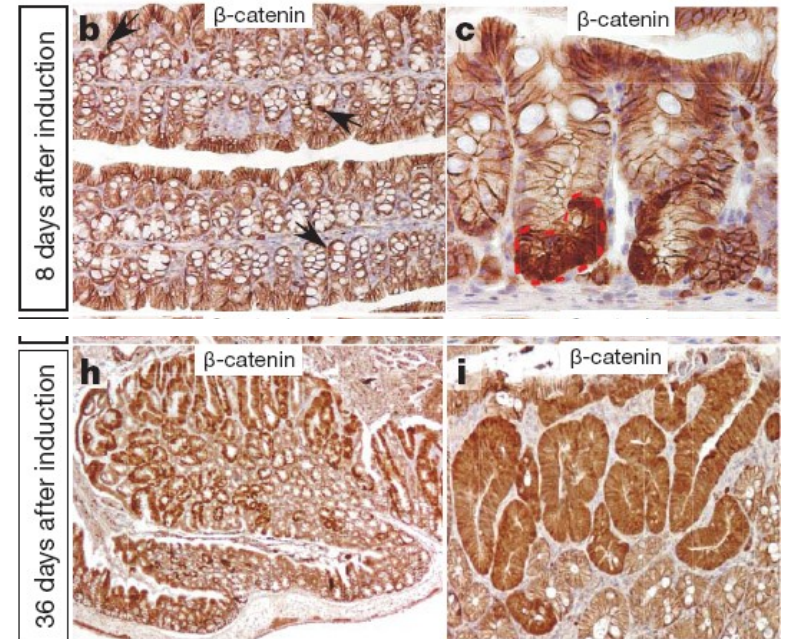
NATURE | Vol 457 | 29 January 2009



Nekontrolovaná aktivace kmenových buněk má fatální následky

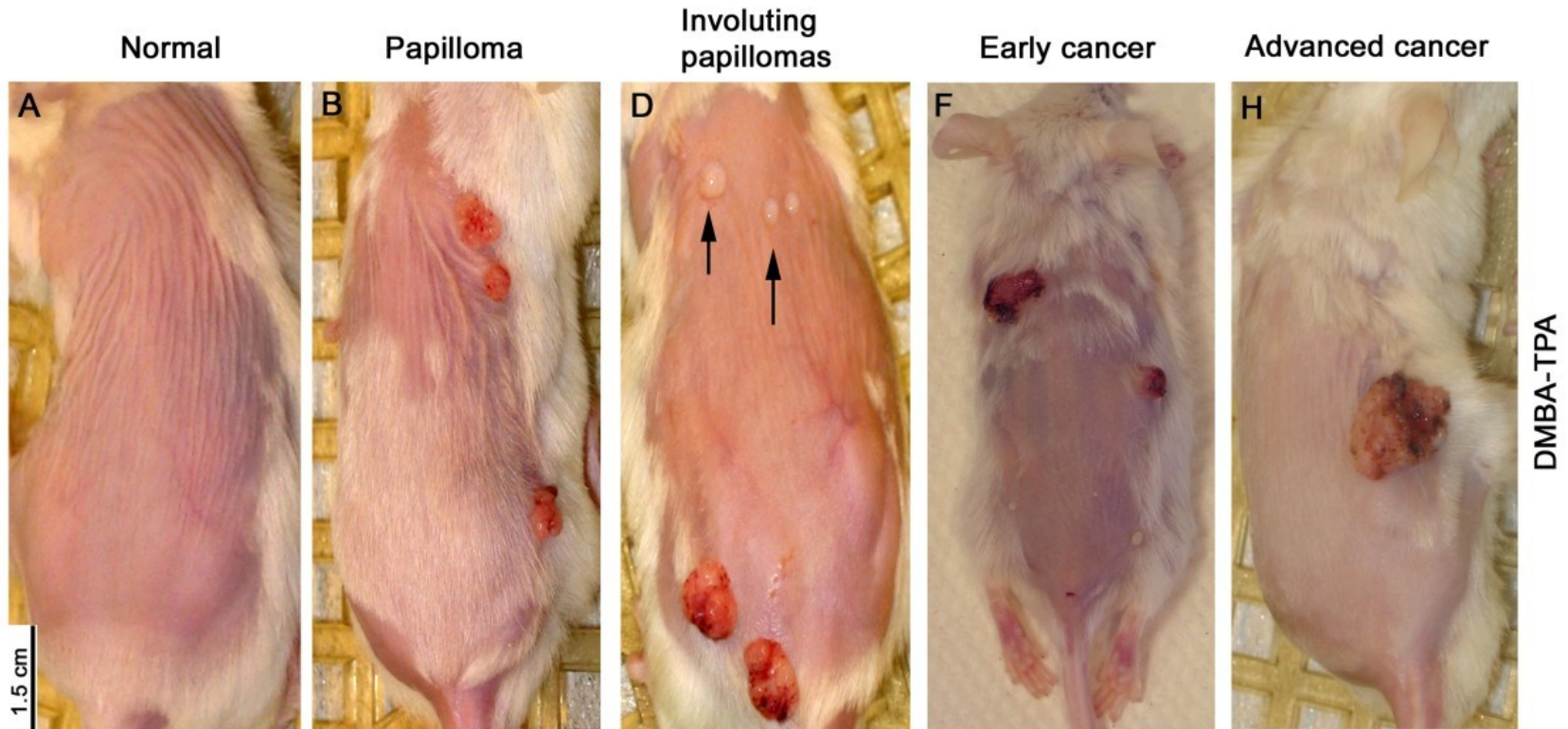


NATURE | Vol 457 | 29 January 2009



DMBA/TPA-induced skin carcinogenesis

- benign papillomas, which in some cases progress into squamous cell carcinoma (SCC)



DMBA/TPA-induced skin carcinogenesis

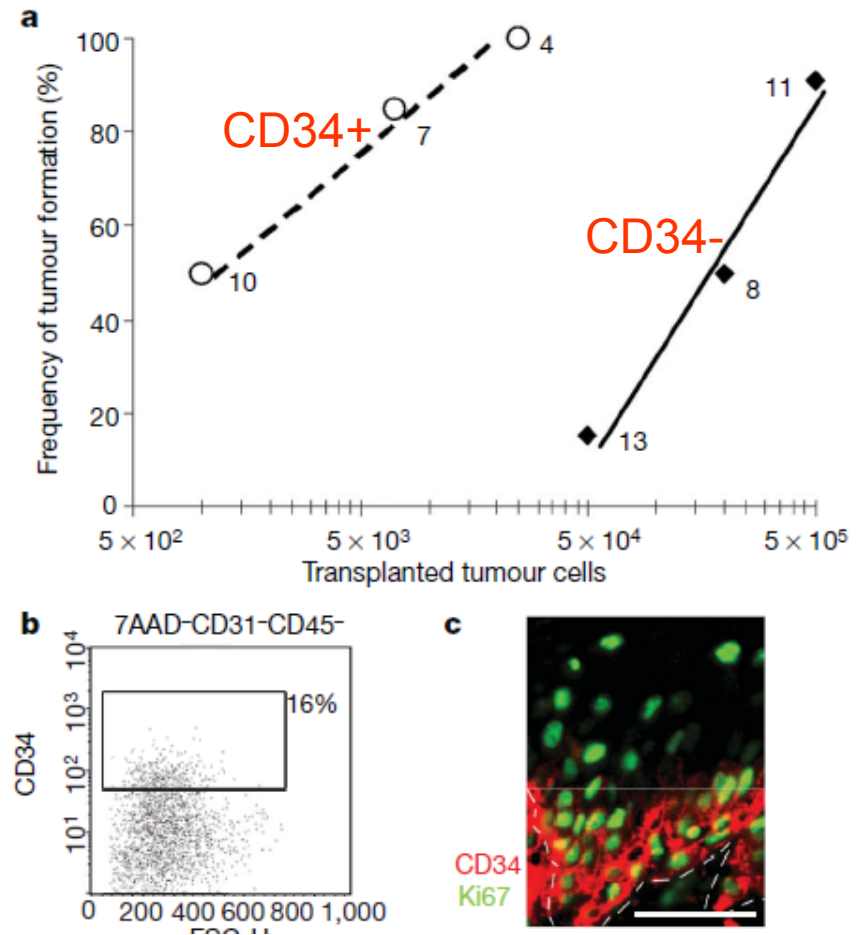
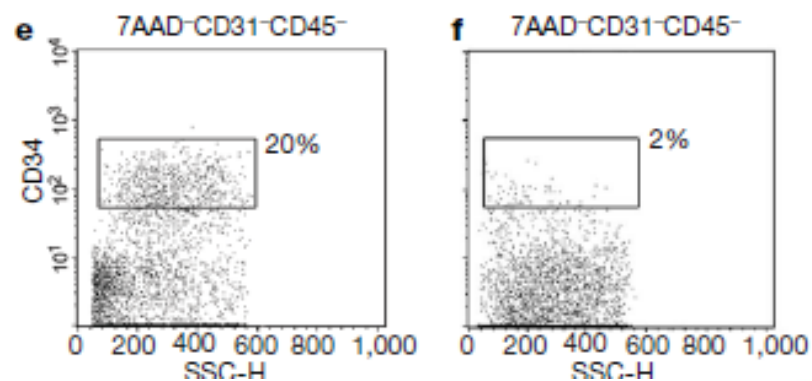
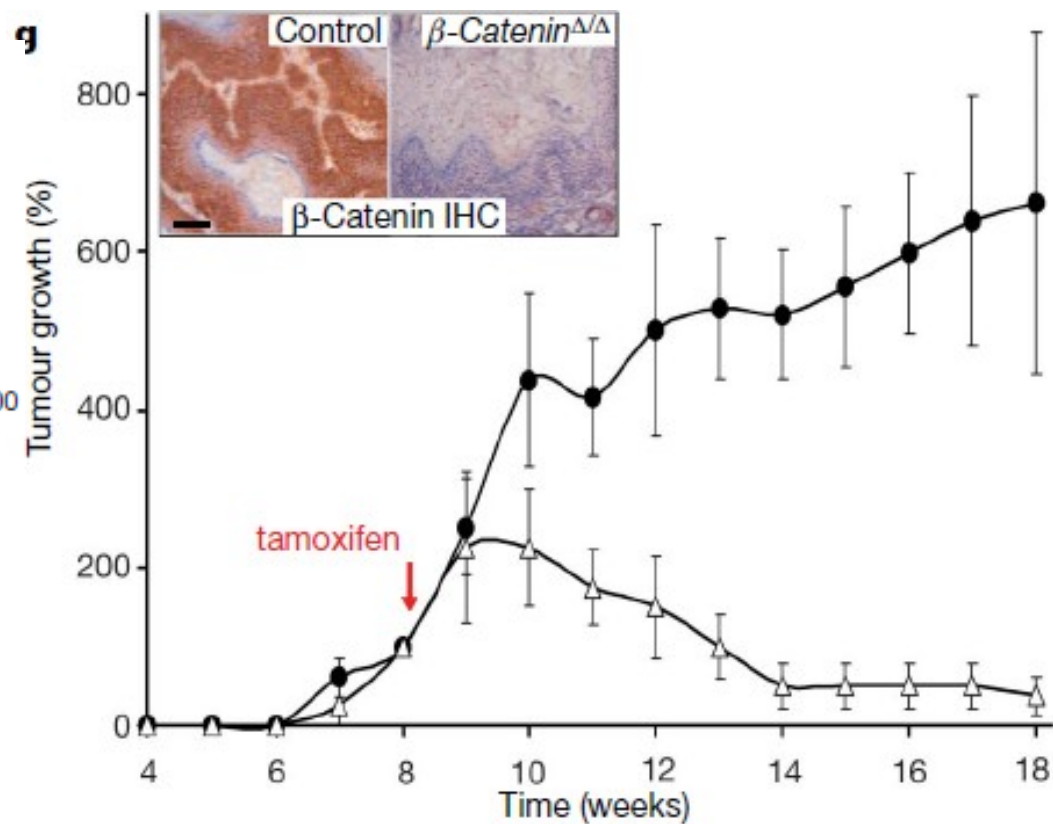


Figure 2 | Cancer stem cells efficiently initiate secondary tumours that recapitulate the organization of the primary tumour. a, Diagram summarizing the frequency of tumour formation in orthotopic tumour transplants using unsorted cells (filled diamonds) or CD34⁺ cells (open circles) in varying amounts. The *n* value for each point is shown. **b**, Abundance of CSCs (CD34⁺7AAD⁻CD31⁻CD45⁻) in secondary tumours derived from orthotopic transplantations of CD34⁺ cells.



characterized by abundant keratinization. **e, f**, Abundance of CD34⁺ cells in control tumours (**e**) and β -catenin-deficient tumours (**f**) two weeks after induction of deletion. **g**, Tumour regression after tamoxifen-induced β -catenin deletion in established skin tumours ($n = 6$; control (filled circles), $K14$ -creER^{T2}; β -catenin^{+/-}; mutant (open triangles), $K14$ -creER^{T2}; β -catenin ^{Δ/Δ}). Tumour numbers at 8 weeks were set to 100%. Error bars show



Malanchi et al. 2008, Nature

Table 1 The table lists the size of the CSC population in different tumor types as determined by using the indicated markers

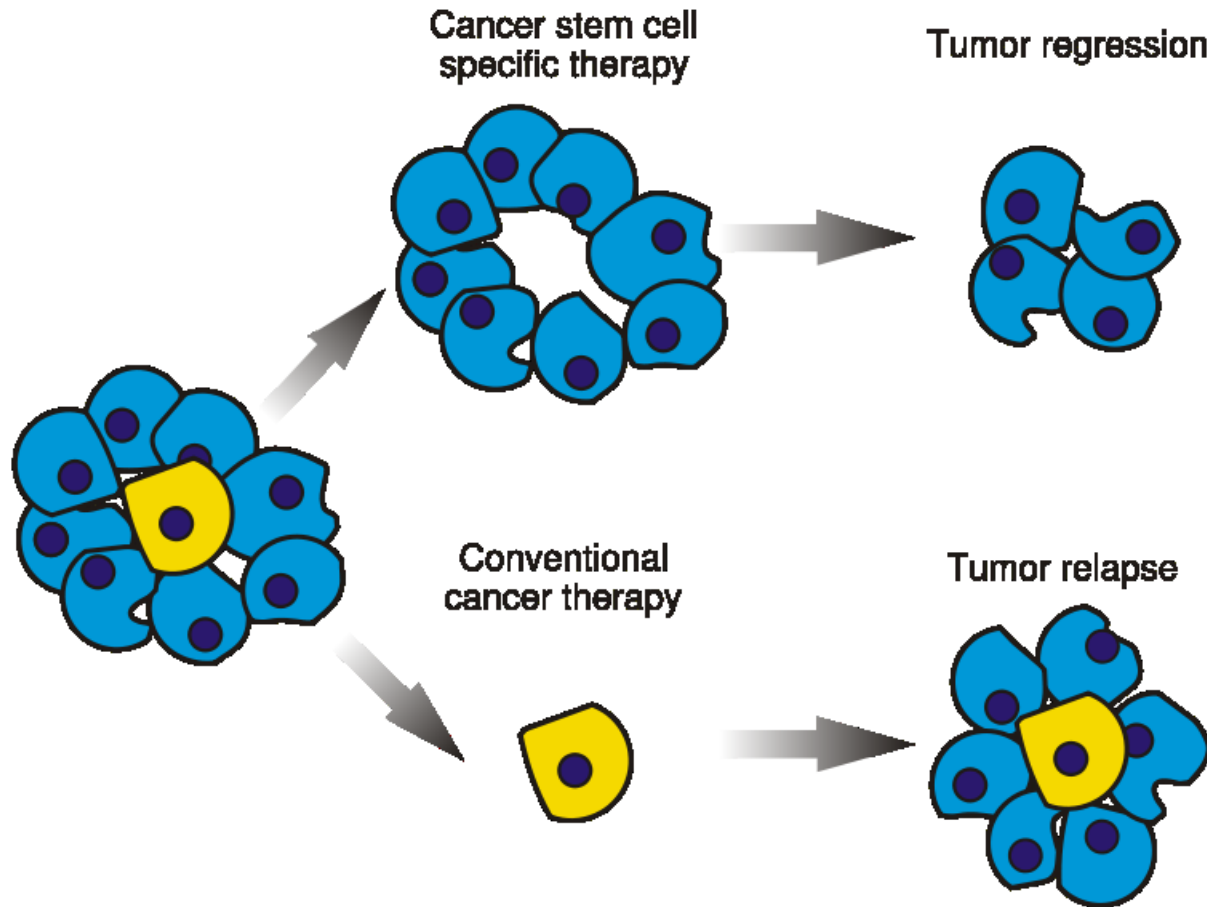
Cancer type	Reference	Stem cell marker	Abundance (%)	Transplanted cells (efficiency in %)
Acute myeloid leukemia	[1]	CD34 ⁺ CD38 ⁻	0.02–1	100 000 (ND)
Breast	[2]	CD44 ⁺ CD24 ^{low}	11–35	5000 (100)
	[2]	CD44 ⁺ CD24 ^{low} ESA ⁺	2.5–5	1000 (100)
	[3]	ALDH ^{high}	3–10	500 (100)
		CD44 ⁺ CD24 ^{low} ALDH ^{high}	0.9–1.2	20 (100)
Brain (medulloblastoma and glioblastoma)	[4]	CD133 ⁺	19–29	100 (100)
Colon	[5]	CD133 ⁺	2–24	100 (25), 500 (83)
Liver	[6]	CD90 ⁺	0.7–6.2	5000 (50)
Lung	[7]	CD133 ⁺	0.4–7	10 000 (ND)
Melanoma	[8]	ABC B5 ⁺	1.6–20.4	100 000 (50)
Prostate	[9]	CD44 ⁺ α 2 β 1 ^{high} CD133 ⁺	0.1–0.3	ND
	[10]	CD44 ⁺ CD24 ^{low}	ND	100 (ND)
Pancreas	[11]	CD44 ⁺ CD24 ⁺ ESA ⁺	0.2–0.8	100 (50) ^a
Head and neck SCC	[12]	CD44 ⁺	10–35	5000–10 000 (50)
Skin SCC ^b	[13 ^{**}]	CD34 ⁺	13–20	1000 (50)

The minimal number of cells inducing secondary tumor formation upon transplantation is included, as well as the efficiency of tumor formation with this number of cells.

^a Some growth from non-CSC population.

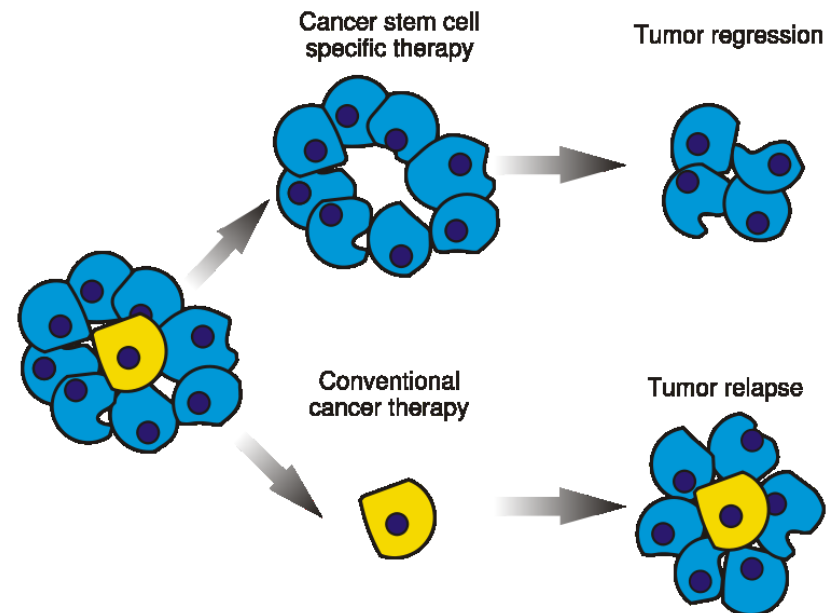
^b Mouse; ND, not determined; SCC, squamous cell carcinoma.

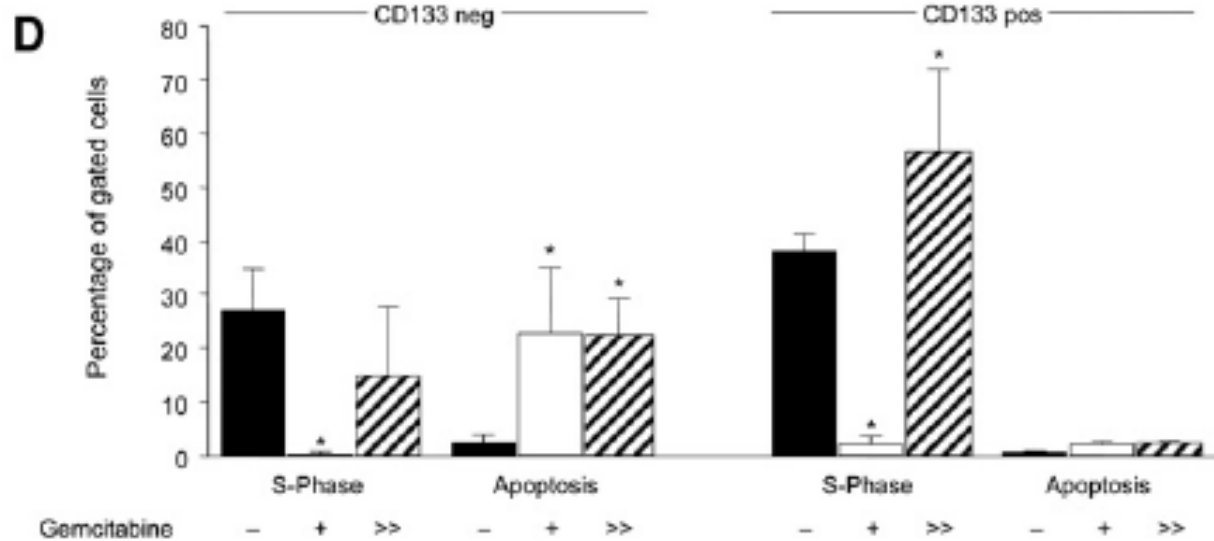
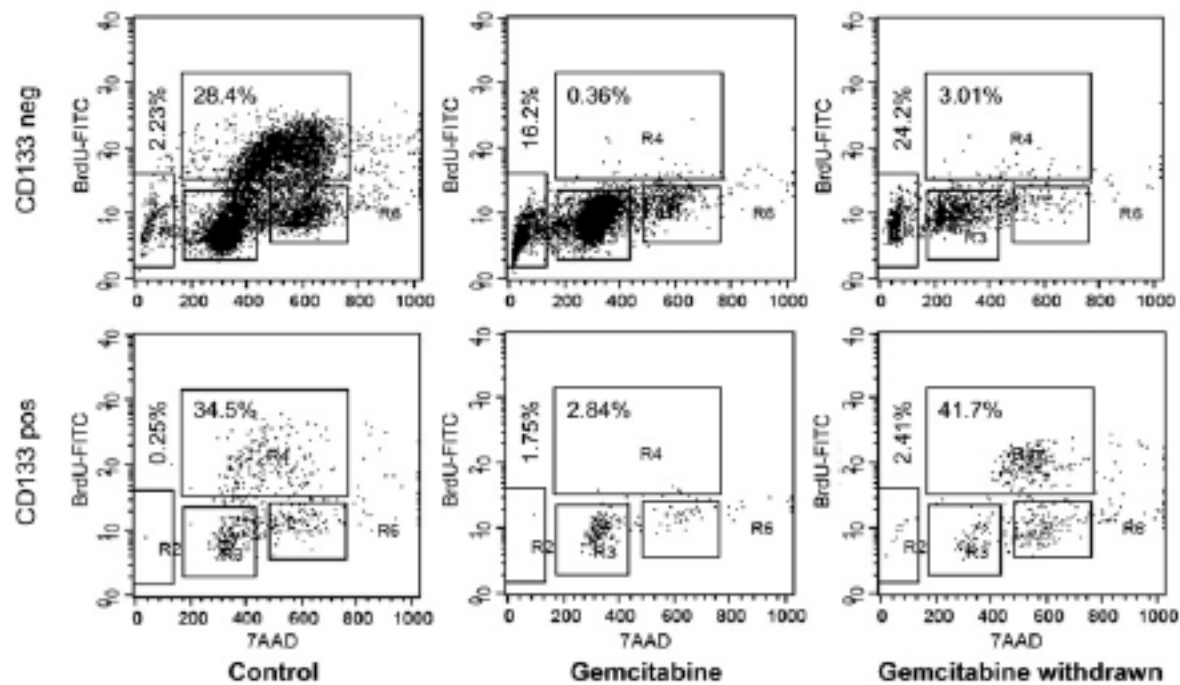
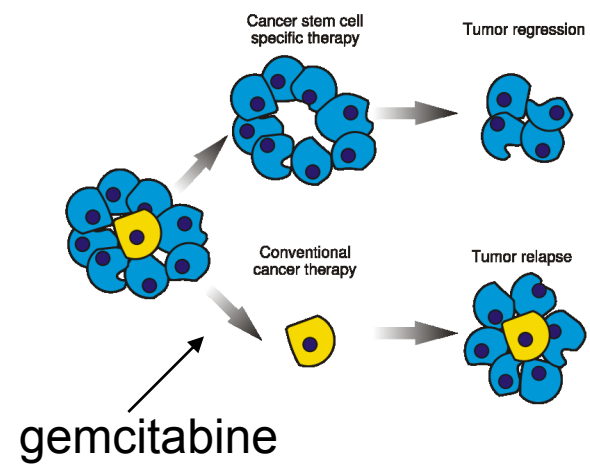
Cancer stem cell based therapy



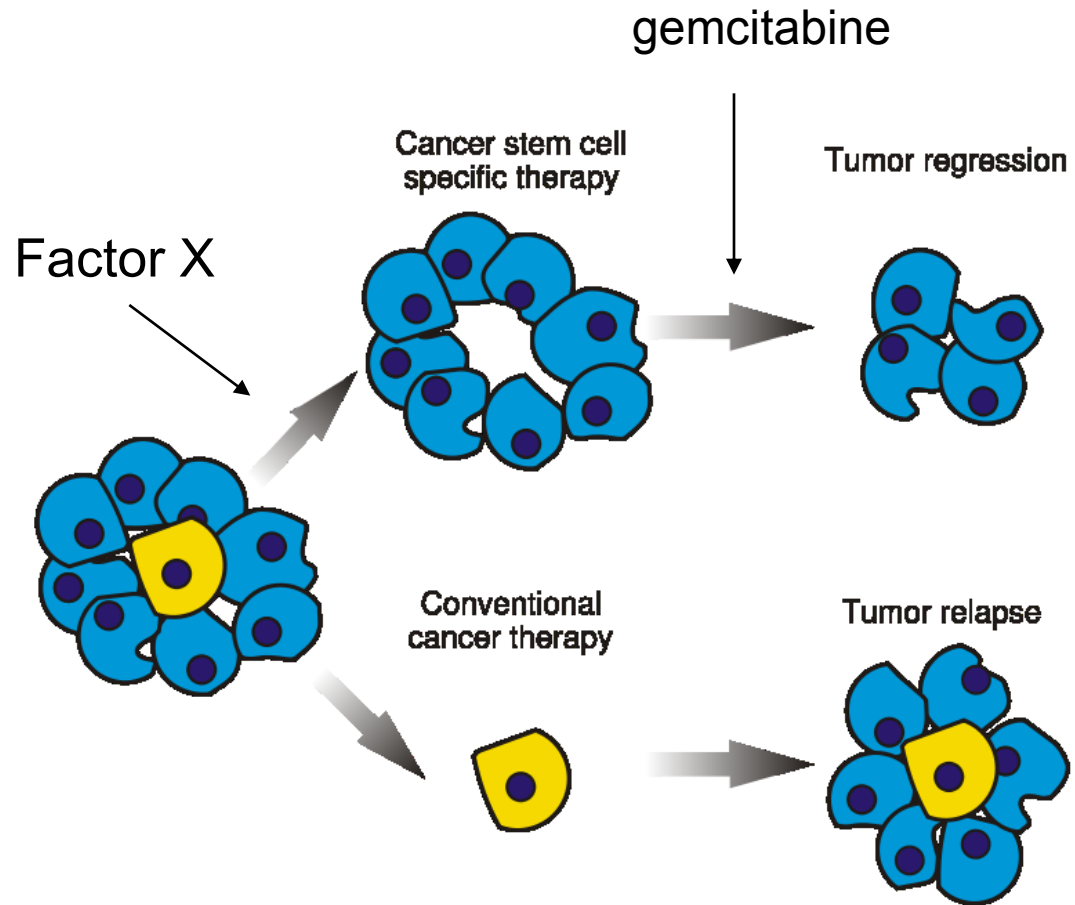
Cancer stem cell based therapy - naděje pro nemocné s nádorem slinivky?

- Pancreatic adenocarcinoma - čtvrtý nejčastější důvod úmrtí u pacientů nádorových onemocnění
- Median survival - 4-6 months
- 5-year survival - 1%
- Treated with gemcitabine - does not work





Terapie budoucnosti?



D

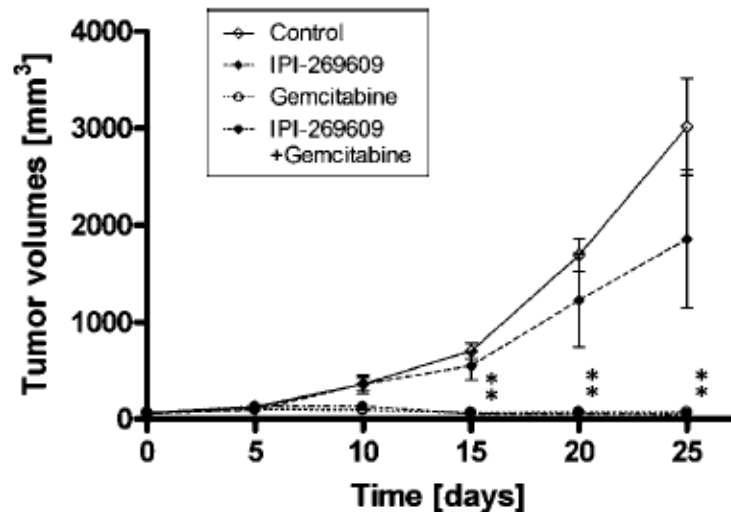
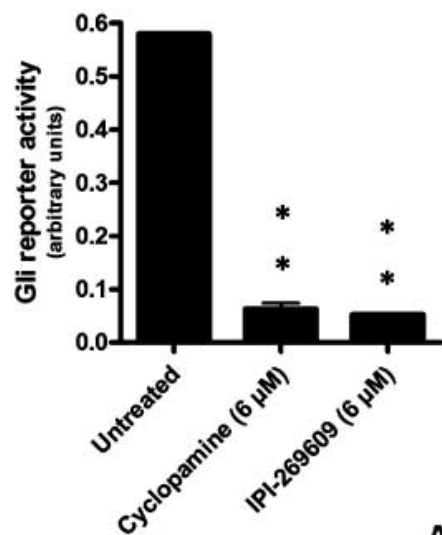
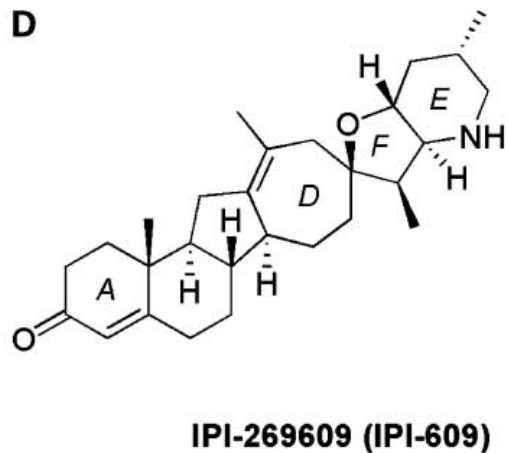
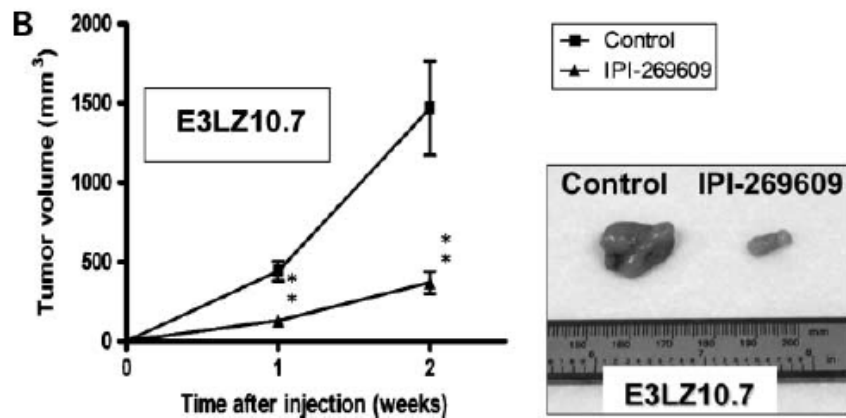
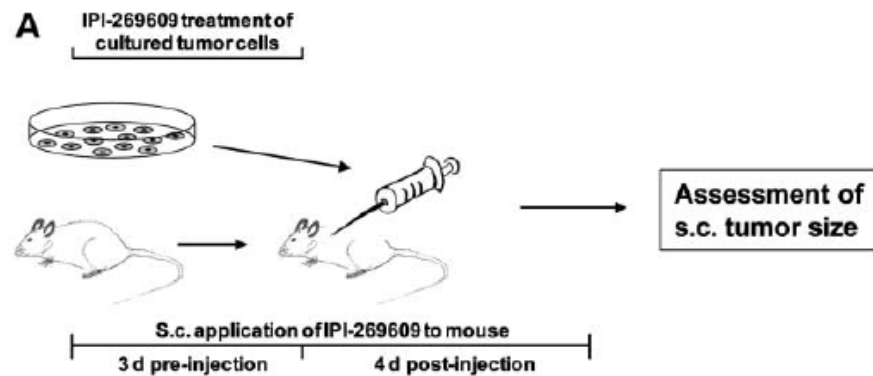
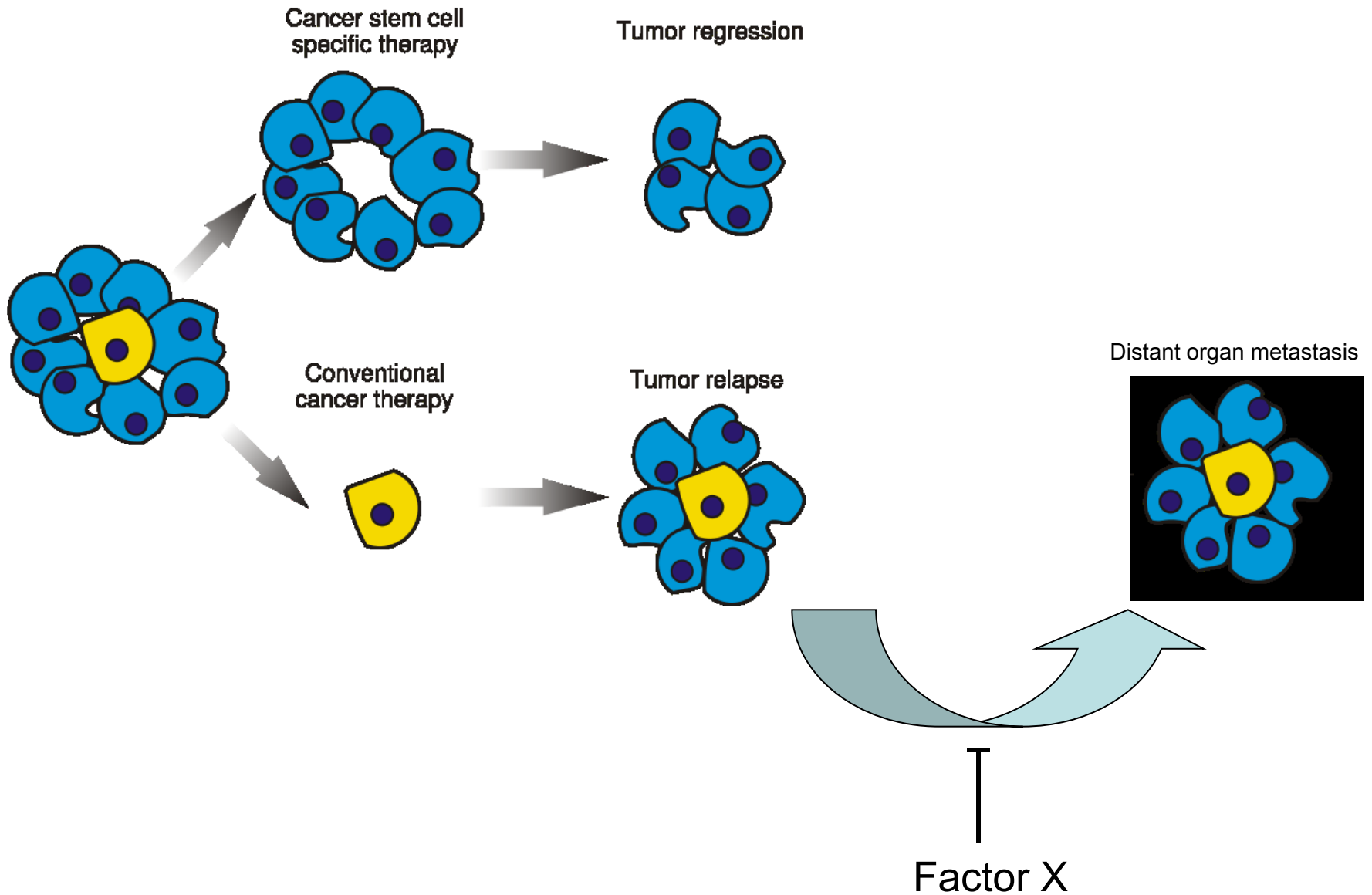


Table 2. Numbers of animals with orthotopic Capan-1 xenografts in which metastases to distant organ sites were found

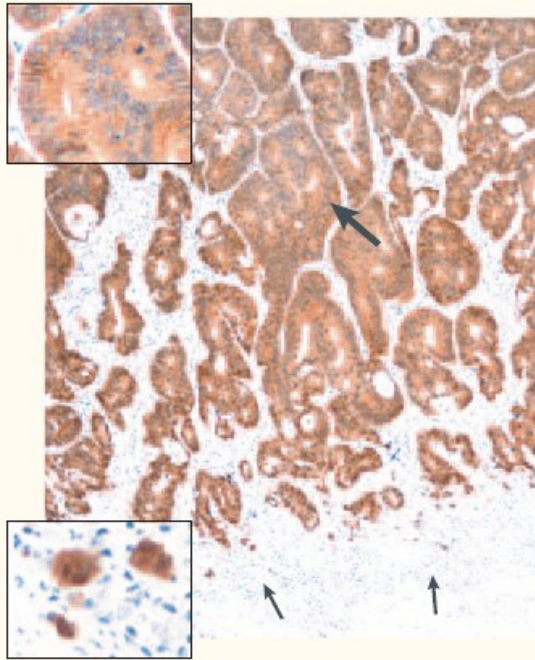
Group	Control, n (%)	IPI-269609, n (%)
No. animals	5	5
Lymph nodes	4 of 5 (80)	2 of 5 (40)
Spleen	5 of 5 (100)	0 of 5 (0)
Liver	4 of 5 (80)	0 of 5 (0)
Intestine	5 of 5 (100)	0 of 5 (0)
Lungs	1 of 5 (20)	0 of 5 (0)
Peritoneum	1 of 5 (20)	0 of 5 (0)
Kidneys	1 of 5 (20)	0 of 5 (0)



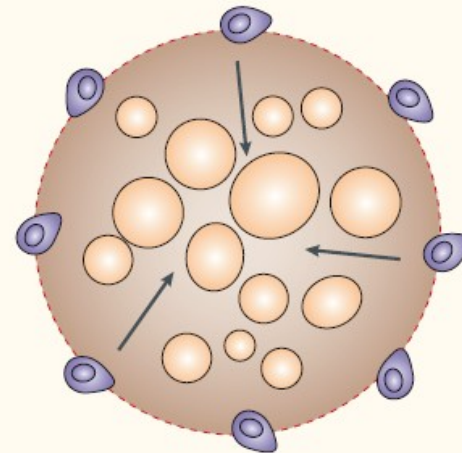
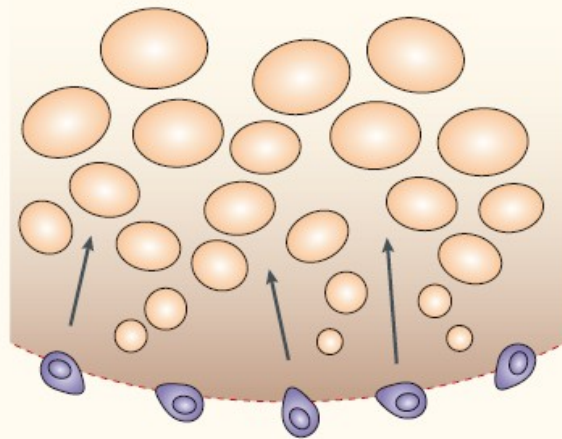
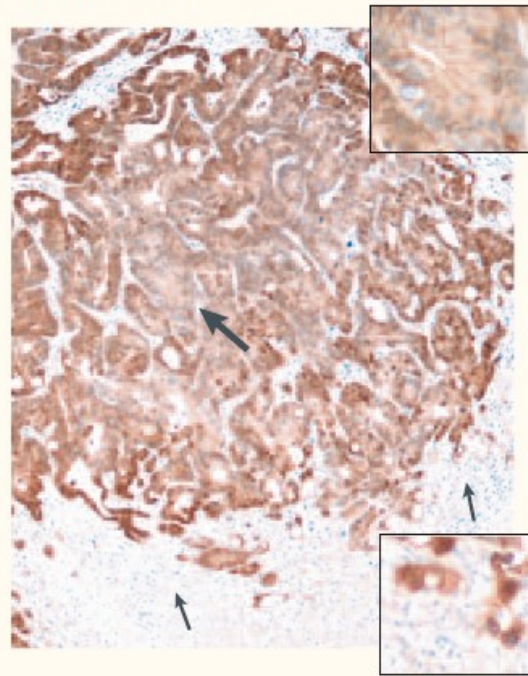
Terapie budoucnosti?





Primary carcinoma




Liver metastasis



 Dedifferentiated tumour cells with strong nuclear β -catenin expression

 Direction of differentiation

 Differentiated tumour areas

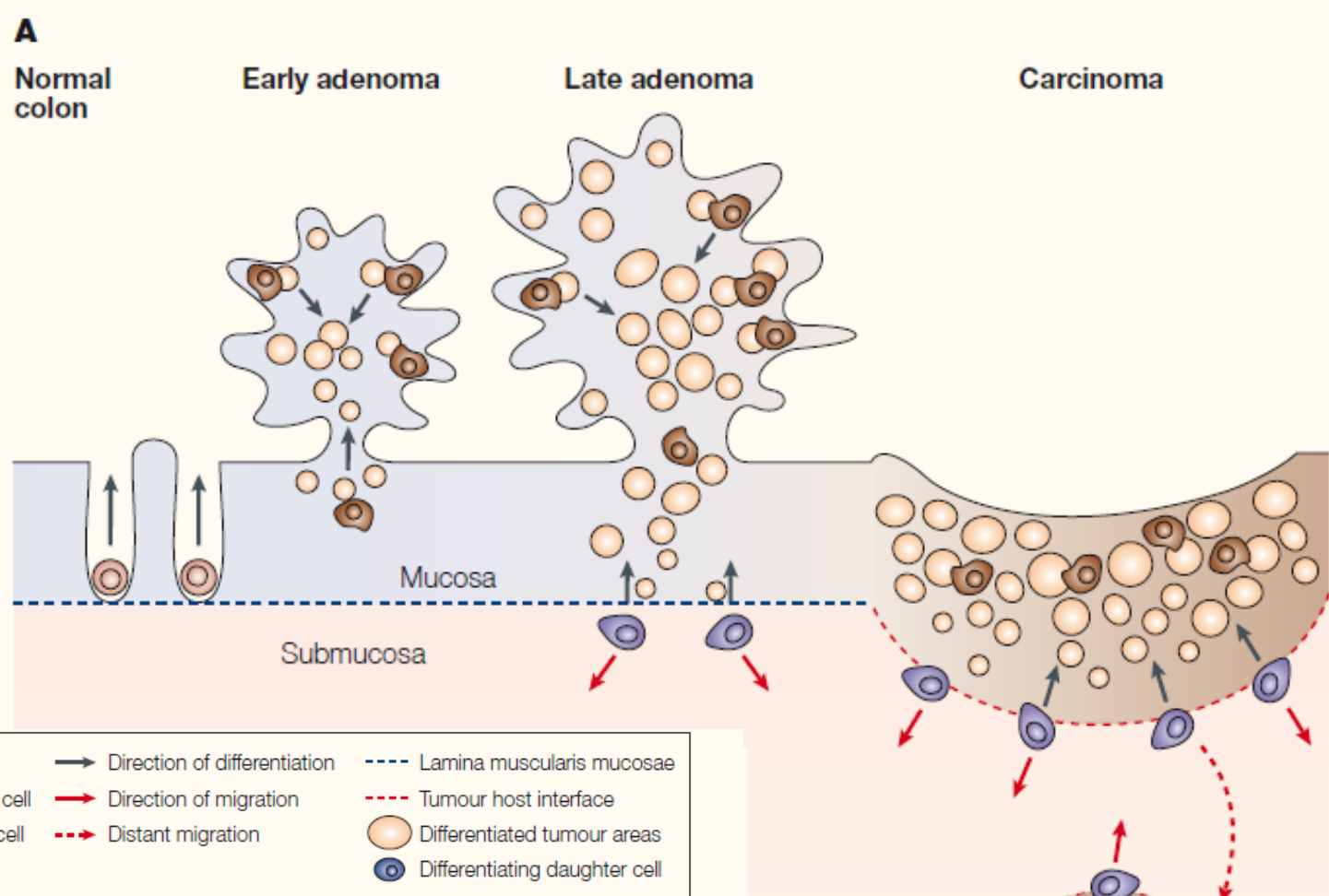
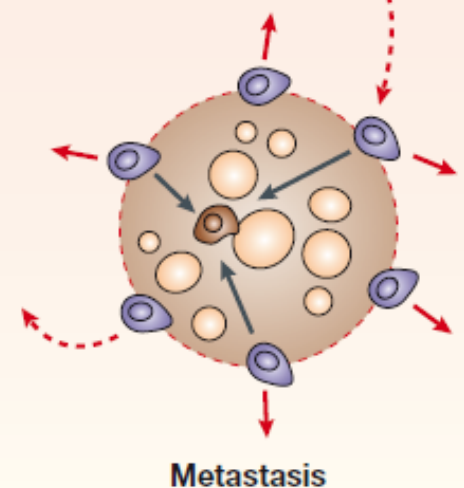
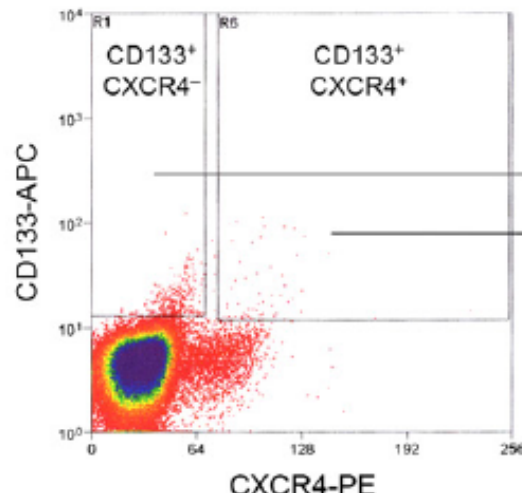


Figure 4 | **The migrating cancer stem (MCS)-cell concept.** **A** | Normal stem cells are located in basal crypt areas of normal colon mucosa. Stationary cancer stem (SCS)-cells are embedded in benign adenomas and might still be detectable in differentiated central areas of carcinomas and metastases (corresponding to phase I, see FIG. 3). A decisive step towards malignancy is the induction of epithelial to mesenchymal transition (EMT) (corresponding to phase II, see FIG. 3) in tumour cells, including SCS-cells, which now become mobile, migrating cancer stem (MCS)-cells. This step could be activated by aberrant environmental signals (in late stage colorectal adenomas this would correlate with the crossing of the border between the mucosa and the submucosa (lamina muscularis mucosae)). **B** | Detailed view of the potential function of MCS cells in carcinomas and metastases. MCS cells divide assymmetrically; one daughter cell starts proliferation and differentiation (a). The remaining MCS cell either migrates a short distance before undergoing a new asymmetric division, thereby adding mass to the primary tumour (b), or eventually starts long-range dissemination through blood or lymphatic vessels and produces a metastasis after subsequent asymmetric divisions at its new location (c). Therefore, the basic mechanisms are the same for primary carcinomas and metastases.



Metastasis driving cancer stem cells: proof from cell lines (pancreatic cancer)



Isolation of

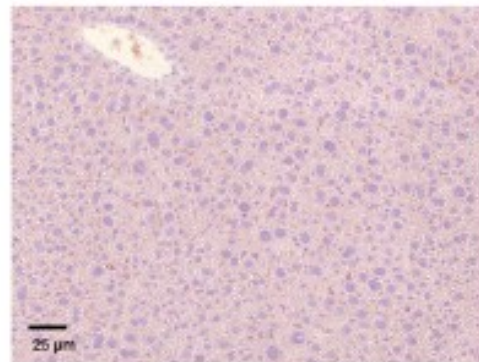
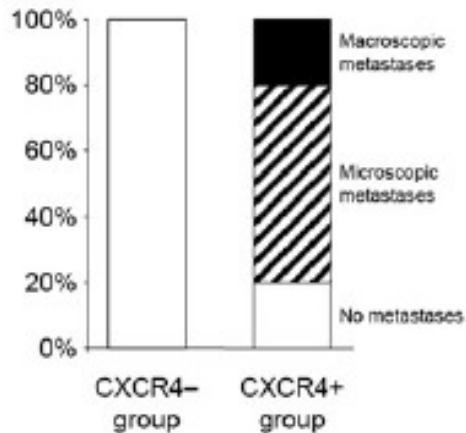
Noninvasive CD133⁺ CXCR4⁻

Highly invasive CD133⁺ CXCR4⁺

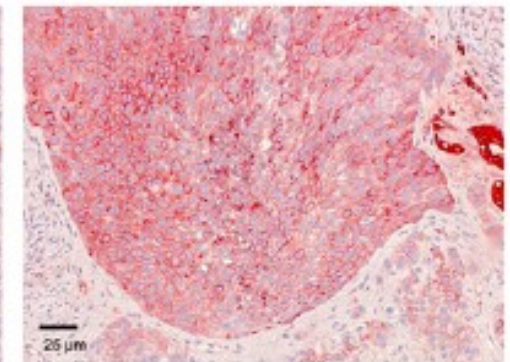
CXCR4⁻ group
(10^3 cells)

CXCR4⁺ group
(each population 5×10^2 cells)

D



CXCR4⁻ group



CXCR4⁺ group

SDF1/CXCL12 - chemokin, ligand exprimovaný v plicích, játrech, kostní dřeni a lymfatických uzlinách; tj. hlavních cílech metastáz

Metastasis driving cancer stem cells: proof from human tumor (colorectal cancer)

A Subpopulation of CD26⁺ Cancer Stem Cells with Metastatic Capacity in Human Colorectal Cancer

Roberta Pang,^{1,2} Wai Lun Law,³ Andrew C.Y. Chu,² Jensen T. Poon,³ Colin S.C. Lam,¹ Ariel K.M. Chow,² Lui Ng,¹ Leonard W.H. Cheung,¹ Xiao R. Lan,¹ Hui Y. Lan,¹ Victoria P.Y. Tan,¹ Thomas C. Yau,¹ Ronnie T. Poon,^{2,3} and Benjamin C.Y. Wong^{1,2,*}

Case	No. cells injected	unsorted	CD133 ⁺				CD133 ⁻			
			CD26 ⁺ CD44 ⁺	CD26 ⁺ CD44 ⁻	CD26 ⁻ CD44 ⁺	CD26 ⁻ CD44 ⁻	CD26 ⁺ CD44 ⁺	CD26 ⁺ CD44 ⁻	CD26 ⁻ CD44 ⁺	CD26 ⁻ CD44 ⁻
Metastatic tumor CD133 ⁺ CD44 ⁺ CD26 ⁺										
	1 x 10 ³	0/0(0)	3/4(4)	1/1(1)	1/1(0)	1/2(0)	3/3(3)	1/1(1)	0/1(0)	0/0(0)
	1 x 10 ⁴	0/0(0)	3/4(4)	2/2(2)	2/1(0)	2/1(0)	3/4(4)	1/2(2)	2/2(0)	0/0(0)
	1 x 10 ⁶	2/2(2)	4/4(4)	2/3(3)	2/3(0)	3/4(0)	2/2(2)	3/4(4)	ND	0/0(0)

Dissociated cells were isolated for 9 different cell subpopulations and implanted into mice subcutaneously or orthotopically (4 animals in each group). Tumor formation was observed for both groups, and animals in the orthotopic implantation group were further observed for development of liver metastasis. Hence, the first two numbers in each cell represents the number of mice with subcutaneous and orthotopic tumor formation, respectively. The third number (in parentheses) refers to the number of animals with liver metastasis developed from the orthotopic implantation group. No liver metastasis was observed in mice with subcutaneous implantation.